

Thanks to

Marta Álvarez for making possible my participation in this project, and for introducing me to the world of chemical oceanography.

Noelia, for all the time she dedicated to me, and for showing how to be a great leader even when external organization doesn't help.

Moisés for finding the time to review my words and meet with me despite his very complicated schedule.

The Maria S. Merian crew for making my time on-board an amazing experience.

The scientific members on board for all the knowledge and advice acquired from them, as well as all the shared free time and lack of sleep.

Elisa, for adopting me as her little 'padawan'.

The IEO for allowing me to use its laboratories and other facilities.

My family for all the support they always give me.

My friends for standing next to me through all the stress time and helping me to release it by having fun.

Contents

Abbreviations	5
Short definitions of oceanographic terms and translation	6
Abstract	7
Resumen.....	8
Resumo.....	9
Timeline.....	10
1. Introduction	11
1.1. CO ₂ chemistry in the ocean	11
The carbonate system	11
pH	12
Total alkalinity	13
Dissolved Inorganic Carbon.....	14
Carbonate Ion.....	14
Carbon cycle in the ocean	14
1.2. The Mediterranean Sea.....	16
1.3. Why CO ₂ in the Mediterranean Sea	19
1.4. Med-SHIP program.....	19
MSM72	20
2. OBJECTIVES OF TFG	23
3. METHODOLOGICAL FUNDAMENTALS.....	25
3.1. Determination of [H ⁺] concentration	25
Fundaments of spectrophotometric determination of pH	25
ΔR Correction	28
3.2. TA determination in seawater.....	29
3.3. DIC determination in seawater	30
3.4. Determination of CO ₃ ²⁻	32
4. WORK MADE AT SEA	33
4.1. Organization	33
4.2. pH measurements	35
Sampling.....	35
Analysis procedure and equipment	35
Quality control.....	36
4.3. TA measurements	39

Sampling.....	39
Analysis procedure and equipment	39
Quality control.....	41
4.4. DIC measurements.....	45
Sampling.....	45
Analysis procedure and equipment	45
Quality control.....	46
4.5. CO ₃ ²⁻ measurements	49
Sampling.....	49
Analysis procedure and equipment	49
Quality control.....	49
5. RESULTS AND DISCUSSION.....	51
5.1. pH controversy: measurements with pure vs. unpurified m-cresol	51
5.2. CO ₂ internal consistency	53
DIC	53
CO ₃ ²⁻	54
5.1. Basin wide vertical distributions in relation to water masses	55
Salinity, temperature and oxygen.....	55
CO ₂ variables	57
6. CONCLUSIONS	61
APPENDIX	62
Bibliography	64

Abbreviations

AW	Atlantic Waters
CA	Carbonate alkalinity
CDOM	Colored Dissolved Organic Mater
CRM	Certified Reference Material
CTD	Conductivity, Temperature and Depth
DIC	Dissolved Inorganic Carbon
DOC	Dissolved Organic Carbon
GO-SHIP	Global Ocean Ship-Based Hydrographic Investigations Program
IEO	Instituto Español de Oceanografía
LIW	Levantine Intermediate Waters
m-CP	Meta Cresol Purple
MedSea	Mediterranean Sea
PA	Practical alkalinity
R/V	Research Vessel
TA	Total alkalinity
THC	Thermohaline Circulation
WOCE	World Ocean Circulation Experiment
St	Station

Short definitions of oceanographic terms and translation

Basin	<i>Wide natural or artificial hollow area covered with water. (Cuenca)</i>
Bathymetry	<i>Topography of ocean's floors. (Batimetría)</i>
Cruise	<i>Oceanographic campaign, research journey on board a ship. (Campaña oceanográfica)</i>
Freshwater	<i>Non-saline water. (Agua dulce)</i>
Vessel	<i>Ship. (Buque)</i>
Niskin	<i>A special type of sampling bottle that can be sunk into the ocean to get seawater from a given depth.</i>
Rosette	<i>Sampling device that carries Niskin bottles (Roseta)</i>

Abstract

The Mediterranean Sea is a very interesting area from a political, social, economic and scientific point of view, because of its location and the activities developed around it, its size and its physicochemical properties. Nevertheless, it wasn't until 2011, with the creation of the MED-SHIP program, that world-wide ocean studies took it into consideration. One of the scopes of this program was to monitor the evolution of its biogeochemical properties, therefore, similar oceanographic cruises should be conducted along the years.

In March of 2018 one of these cruises, the MSM72, took place. This end-of-degree thesis introduces the chemistry of the carbonate system in seawater and the importance of its study in the Mediterranean Sea. In addition, this work summarizes the data obtained by the chemical oceanography group in charge of the measurements for the CO₂ system's variables (pH, Total Alkalinity, Dissolved Inorganic Carbon and carbonate ion) during the MSM72 cruise as well as the analysis procedures, from the sampling to the resulting information.

Resumen

El Mar Mediterráneo es una zona muy interesante desde un punto de vista político, social, económico y científico debido a su ubicación y las actividades desarrolladas en torno a él, su tamaño y sus propiedades fisicoquímicas. Sin embargo, no fue hasta 2011, con la creación del programa MED-SHIP que los grandes estudios internacionales del océano lo incluyeron. Uno de los objetivos de este programa es monitorizar la evolución de las propiedades biogeoquímicas de este mar, de manera que varias campañas oceanográficas similares deberían llevarse a cabo a lo largo de los años.

En marzo de 2018, tuvo lugar una de estas campañas, la MSM72. Este TFG introduce la química del sistema del carbonato en agua de mar y la importancia de su estudio en el Mar Mediterráneo. Además, este trabajo resume los datos obtenidos por el grupo de química encargado de medir las variables del sistema del CO₂ (pH, Alcalinidad Total, Carbono Inorgánico Disuelto e ion carbonato) durante la campaña MSM72, así como explica el procedimiento de los análisis desde el muestreo hasta la obtención de información.

Resumo

O Mar Mediterráneo é unha zona moi interesante dende un punto de vista político, social, económico e científico debido á súa ubicación e as actividades desenvoltas no seu redor, o seu tamaño e as súas propiedades fisicoquímicas. Non obstante, non foi ata o 2011, coa creación do programa MED-SHIP que os grandes estudos internacionais do océano o tiveron en conta. Un dos obxectivos deste programa é monitorizar a evolución das propiedades bioxeoquímicas deste mar, de maneira que varias campañas oceanográficas similares deberían levarse a cabo ao longo dos anos.

En marzo de 2018, tivo lugar unha destas campañas, a MSM72. Neste TFG introdúcese a química do sistema do carbonato en auga de mar e a importancia do seu estudo no Mar Mediterráneo. Ademais, este traballo resume os datos obtidos polo grupo de química encargado de medir as variables do sistema do CO₂ (pH, Alcalinidad Total, Carbono Inorgánico Disuelto e ión carbonato) durante a campaña MSM72, así como explicar o procedemento dos análisis dende o muestreo ata a obtención de información.

Timeline

Febrero						
L	M	X	J	V	S	D
			1	2	3	4
5	6	7	8	9	10	11
12	13	14	15	16	17	18
19	20	21	22	23	24	25
26	27	28				






Marzo						
L	M	X	J	V	S	D
			1	2	3	4
5	6	7	8	9	10	11
12	13	14	15	16	17	18
19	20	21	22	23	24	25
26	27	28	29	30	31	

Abril						
L	M	X	J	V	S	D
						1
2	3	4	5	6	7	8
9	10	11	12	13	14	15
16	17	18	19	20	21	22
23	24	25	26	27	28	29
30						

Mayo						
L	M	X	J	V	S	D
	1	2	3	4	5	6
7	8	9	10	11	12	13
14	15	16	17	18	19	20
21	22	23	24	25	26	27
28	29	30	31			

Junio						
L	M	X	J	V	S	D
				1	2	3
4	5	6	7	8	9	10
11	12	13	14	15	16	17
18	19	20	21	22	23	24
25	26	27	28	29	30	

Julio						
L	M	X	J	V	S	D
						1
2	3	4	5	6	7	8
9	10	11	12	13	14	15
16	17	18	19	20	21	22
23	24	25	26	27	28	29
30	31					

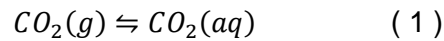
-  Preparation of cruise
-  Oceanographic cruise
-  pH data treatment
-  Chloridric acid titrations
-  Writing

Introduction

1.1. CO₂ chemistry in the ocean

The carbonate system

Carbon dioxide, CO₂, is one of the most abundant gas in the Earth's atmosphere and a very important greenhouse gas. Gaseous CO₂ in the atmosphere is dissolved in the ocean establishing an equilibrium related to Henry's law. According to this law, the solubility of a gas is proportional to its partial pressure above the liquid (2).



Thermodynamic equilibrium between atmospheric and dissolved CO₂ in the water surface. The equilibrium constant, K₀ of the process is temperature and salinity dependent.

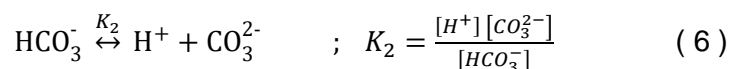
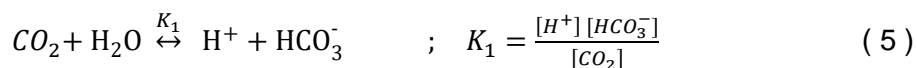
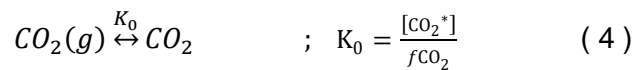
$$S_i = k \cdot P_i \quad (2)$$

Henry's law, where S_i is the solubility of gas i, k is the Henry's constant for "i" in a specific solvent, and P_i the partial pressure of i above the liquid.

The dissolved CO₂(aq) produces carbonic acid (H₂CO₃), which cannot be chemically separated from the former species, therefore it is usually denoted as either CO₂ or H₂CO₃*.¹ In what follows, we will adopt the first option.

$$[CO_2] = [CO_2(aq)] + [H_2CO_3] \quad (3)$$

This CO₂ is rapidly converted into two more stable and abundant forms: bicarbonate (HCO₃⁻) and carbonate (CO₃²⁻), following the equilibria shown in **Figure 1**.



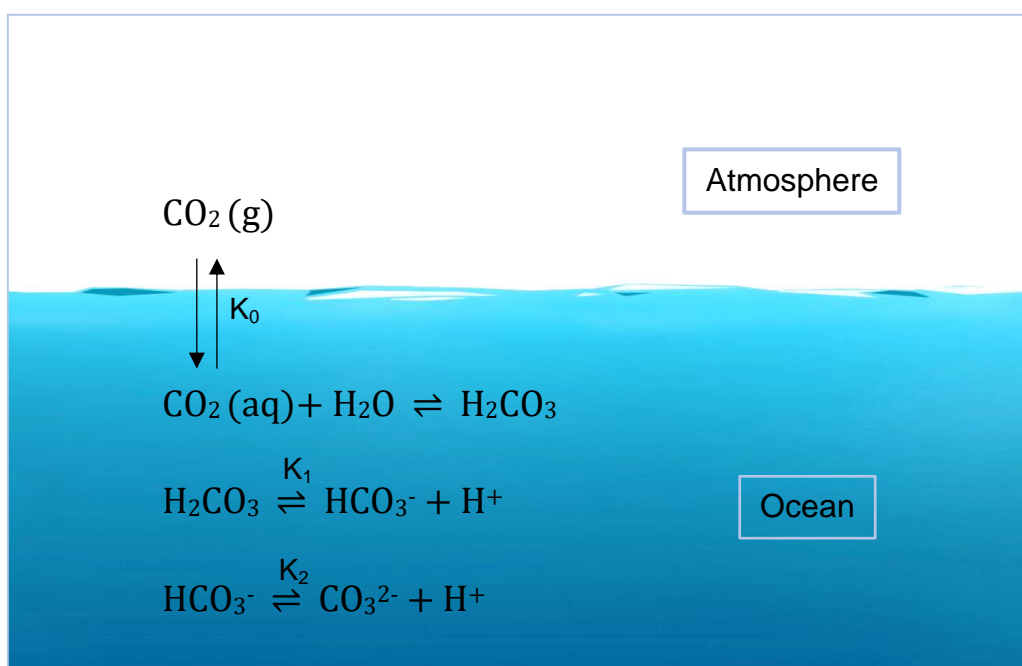


Figure 1. Carbonate system in the ocean. $\text{CO}_2(\text{g})$ in the atmosphere is in exchange with $\text{CO}_2(\text{aq})$ in the ocean. K_0 is Henry's constant, K_1 is the constant for the first deprotonation reaction and K_2 for the second one. At 25°C, with a salinity of 35 and 1 atm pressure, $pK_1=5.86$, $pK_2=8.92$ (values from Zeebe, 2002)¹

Traditionally, the carbonate system in the ocean has been characterized by four measured variables, which combine the chemical species of the CO_2 system (Figure 1 and equations 4, 5 and 6): pH, total alkalinity (TA), total dissolved inorganic carbon (DIC) and fugacity of CO_2 in the gas phase ($f\text{CO}_2$)ⁱ. Recently, the ion carbonate concentration [CO_3^{2-}] started to be measured too.

pH

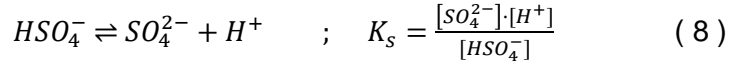
pH is defined as the negative logarithm of the total hydrogen ion activity. In the context of sea water, there are several scales to express pH, depending on which definition of the concentration of hydrogen ions is used.²

The adopted scale in the present work is the so-called “total seawater scale”, which includes the concentration of free hydrogen ions $[\text{H}^+]_F$ and also the total concentration of sulfate ions, $[\text{HSO}_4^-] + [\text{SO}_4^{2-}]$. They have to be taken into account because they interfere in the determination of free hydrogen ions.²

ⁱ Because it is not possible to measure $f\text{CO}_2$ at the IEO and therefore it was not studied during this TFG, I will not explain it in detail.

$$[H^+] = [H^+]_F \left(1 + \frac{[HSO_4^-] + [SO_4^{2-}]}{K_s} \right) \quad (7)$$

Where K_s is the acid dissociation constant for HSO_4^- .³



Note that this scale is based on the adoption of the standard state for seawater in which the activity coefficient, γ_i , is one, and therefore activities, a_i , may be expressed as concentrations [i], in moles/L.²

$$a_i = \gamma_i \cdot [i] \quad ; \quad \gamma \rightarrow 1 \quad ; \quad a_i = [i] \quad (9)$$

Other scales are the Seawater Scale (SWS), which adds fluoride ions to the total hydrogen ion definition; the NBS scale (National Bureau Scale), based on some low ionic strength standards and the free hydrogen ion concentration scale, which does not take into account the participation of any species other than hydrogen ions.

Total alkalinity

Total alkalinity (TA) was first defined as carbonate alkalinity, referred to the charge concentration of carbonic acid anions present in water. Borate and water alkalinity were added to the definition yielding the practical alkalinity, which can be used for most calculations of seawater parameters. Finally, the definition of TA (total alkalinity) was introduced, taking into account a balance of proton donors and acceptors.

The final definition given by Dickson³ was: "amount of hydrogen ions required to neutralize the protons acceptors in 1 kg of seawater"³. It was suggested to consider as proton acceptors the bases formed from weak acids (with $pK > 4.5$ and zero ionic strength at 25°C).

The expression for total alkalinity would then be:

$$TA = [HCO_3^-] + 2[CO_3^{2-}] + [B(OH)_4^-] - [H^+]_F + [OH^-] + [HPO_4^{2-}] + 2[PO_4^{3-}] + [SiO(OH)_3^-] + [HS^-] + 2[S^{2-}] + [NH_3] - [HF] - [H_3PO_4] \quad (10)$$

Small contributors (<1 $\mu\text{mol/kg}$) such as hydroxide, phosphate or silicate are ignored.⁴

Dissolved Inorganic Carbon

The total dissolved inorganic carbon, DIC, TCO_2 or CT, is the sum of all species involved in the thermodynamic equilibria of the carbonate system (**Figure 1**)

$$\text{DIC} = [\text{CO}_3^{2-}] + [\text{HCO}_3^-] + [\text{CO}_2] \quad (11)$$

Note that the term $[\text{CO}_2]$ includes $[\text{CO}_2(\text{aq})]$ and $[\text{H}_2\text{CO}_3]$.⁴

DIC is independent from temperature, salinity and pressure, but the equilibrium constants do depend on these variables, therefore the stoichiometry will differ among samples. In sea water, $[\text{HCO}_3^-]$ is usually a lot greater than the other two concentrations.¹

Carbonate Ion

Historically, the four measurable variables of the carbonate system were pH, TA, DIC and $f\text{CO}_2$, but in the XXI century, the carbonate ion concentration ($[\text{CO}_3^{2-}]$) is considering the fifth measurable variable, as recent studies have demonstrated.⁵⁻⁷

Carbon cycle in the ocean

The distribution of carbon between the ocean and the atmosphere is mainly due to two mechanisms: the physical or solubility pump and the biological pump.⁸

The physical or solubility pump is governed only by thermodynamic and kinetic processes. Usually, solubility of gasses increases with decreasing temperature and is directly proportional to salinity and pressure or depth. Once it is dissolved in surface water, it is later carried to intermediate and deep waters by the thermohaline circulation (THC), which is result of density gradients between different water masses.⁹

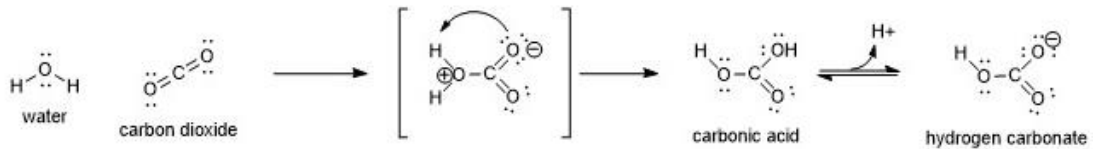
The biological pump is controlled by living organism processes such as production of biological matter and its remineralization. First, primary producers through photosynthesis, transform dissolved CO_2 , light and nutrients into organic matter. The fixed CO_2 becomes part of the food chain, and then most of it falls to the bottom in the form of pellets from excretion and fragments of dead organisms to decompose and is finally re-mineralized to start the cycle again or to remain as sediments.

Most marine organisms live in the upper layers of the ocean, where CO_2 exchange takes place, therefore it seems convenient to study possible changes in the chemistry of surface water, in case it has an impact on the marine ecosystem.¹⁰

Three main direct consequences of CO_2 accumulation in the oceans are:

a) Increasing in CO_2 concentration itself, which may affect directly photosynthetic organisms that need it for fixation.

b) A pH decrease due to the release of a proton during bicarbonate formation from ionization of carbonic acid.



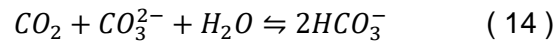
(12)

Most released protons are neutralized by carbonate ion, CO_3^{2-} , so the ocean has a buffering capacity. However, this neutralization may be eventually limited by the availability of the carbonate ion.



(13)

The overall reaction can be written as:



The buffering ability of seawater is due to carbonate ion neutralizing protons and CO_2 forming bicarbonate. The borate ion $\text{B}(\text{OH})_4^-$ provides a similar but less important effect.

c) Decreasing in the concentration of CO_3^{2-} , which may affect precipitation of calcium carbonate by calcifying organisms since the saturation state, Ω is also decreased.¹⁰

$$\Omega = \frac{[\text{Ca}^{2+}][\text{CO}_3^{2-}]}{K_{sp}} \quad (15)$$

(15) Relation between the concentration of the ions and the solubility constant (K_{sp}).

1.2. The Mediterranean Sea

The Mediterranean Sea (MedSea) is a semi-enclosed sea, open to the Atlantic Ocean through the Strait of Gibraltar and surrounded by twenty-one populated countries.

It is composed by two main basins of approximately the same size, the Eastern and the Western, separated by the Strait of Sicily. Each basin is divided in several sub-basins⁹, as it is shown in **Figure 2**.

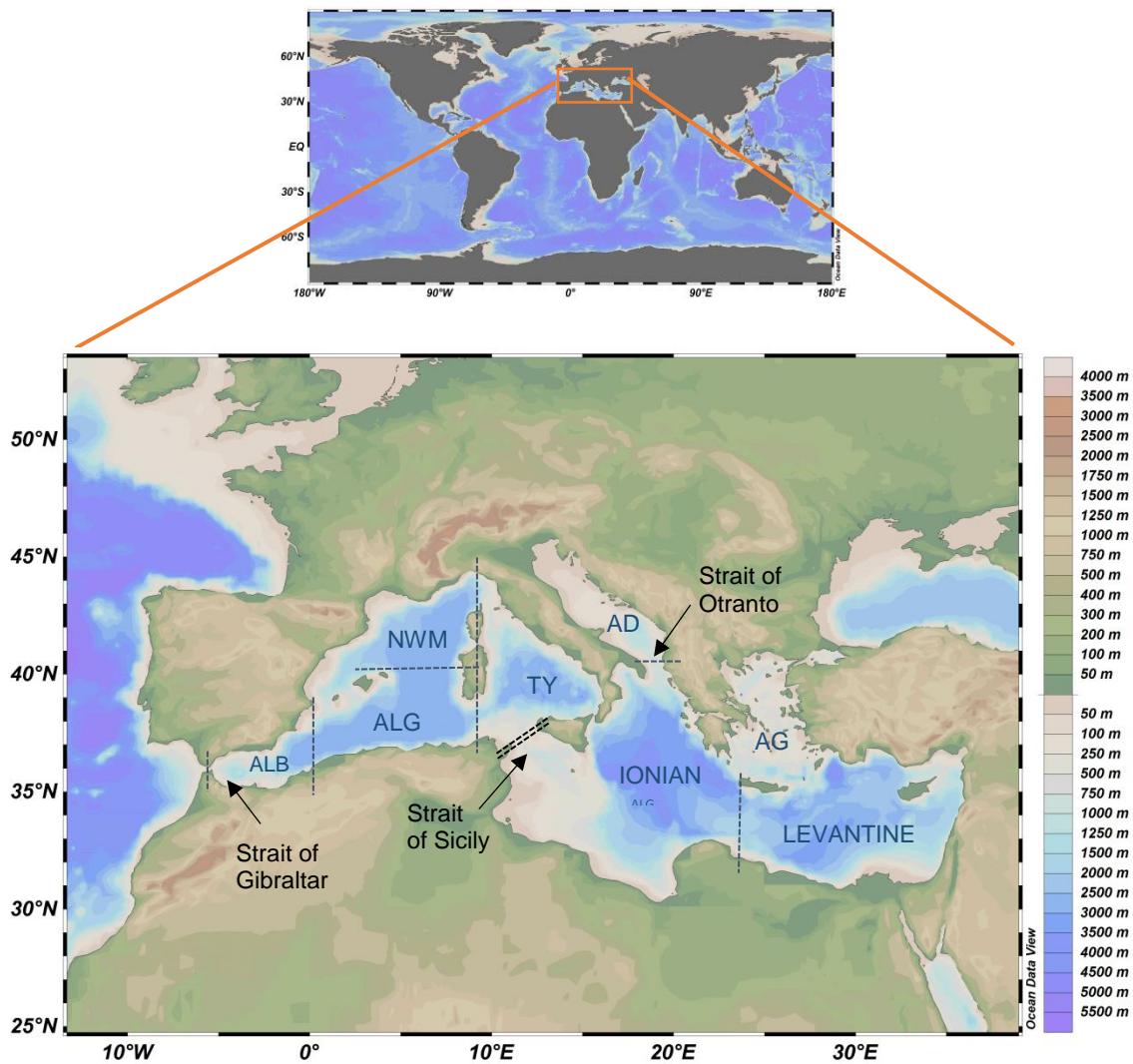


Figure 2. Map of the MedSea with topography and bathymetry. The Western and Eastern basins are separated by the Strait of Sicily. The Western basin is divided in four sub-basins (in dark blue): Alboran (ALB), Algerian (ALG), North-West Mediterranean (NWM) and Thyrrhenian (TY). The Eastern basin, is divided as well in the corresponding sub-basins: Ionian, Adriatic (AD), Aegean (AG) and Levantine. The strait of Gibraltar separates the Mediterranean Sea from the Atlantic Ocean and the Strait of Otranto separates the Ionian and Adriatic sub-basins.

A water mass is defined in oceanography as a large volume of water that may be identified as having a common origin in a certain area. It has a characteristic interval of temperature, salinity and oxygen content values, corresponding to its formation conditions.

They are usually formed by the interaction between water and atmosphere, cooling down and/or an increasing in the salinity of the surface. Once they are formed, water masses sink and settle at a certain depth, depending on their density relative to the surrounding water masses.¹¹

Water masses are called after the place where they are formed and the depth they settle at. Depth intervals are shown in table 1.¹²

Layer	Depth (m)
Upper waters	0-500
Intermediate waters	500-1500
Deep and abyssal waters	1500-bottom

Table 1. Traditional classification of water layers. The deep and bottom waters occupy an important portion of the ocean and they are most of their lifetime isolated from the surface, so the exposure to changes is minimal, and therefore their properties are more stable in time. On the contrary, upper waters are affected by constant variations, altering their salinity and temperature. Taken from Emery, 2003.

The Strait of Gibraltar communicates the MedSea with the Atlantic Ocean, allowing the entrance of a relatively freshwater flux called Atlantic Water (AW), into the Western basin. These water masses increase in density because evaporation in both basins exceeds precipitation yielding high salinity, temperature and density water.⁹ When the AW reaches the Levantine basin, it is denser and more saline, and it conforms the Levantine Intermediate Water (LIW), which flows back to the Atlantic. There is deep water formation in both basins, the Western Mediterranean Deep Water (WMDW) is formed in Lions gulf and the Eastern Mediterranean Deep Water (EMDW) in the Adriatic Sea.¹³

In the beginning of the 90's, the Aegean became the principal deep water formation source, during the so-called Eastern Mediterranean Transient (EMT). A deeper and more saline water mass was formed in the Cretan Sea, the Cretan Deep Water (CDW).¹³

Nowadays, deep water is mainly formed in the Adriatic, as it was before the EMT, but the water is warmer and saltier, more similar to that constituted during the EMT.¹³In **Figure 3**, the main water masses formation and its distribution at the MedSea are

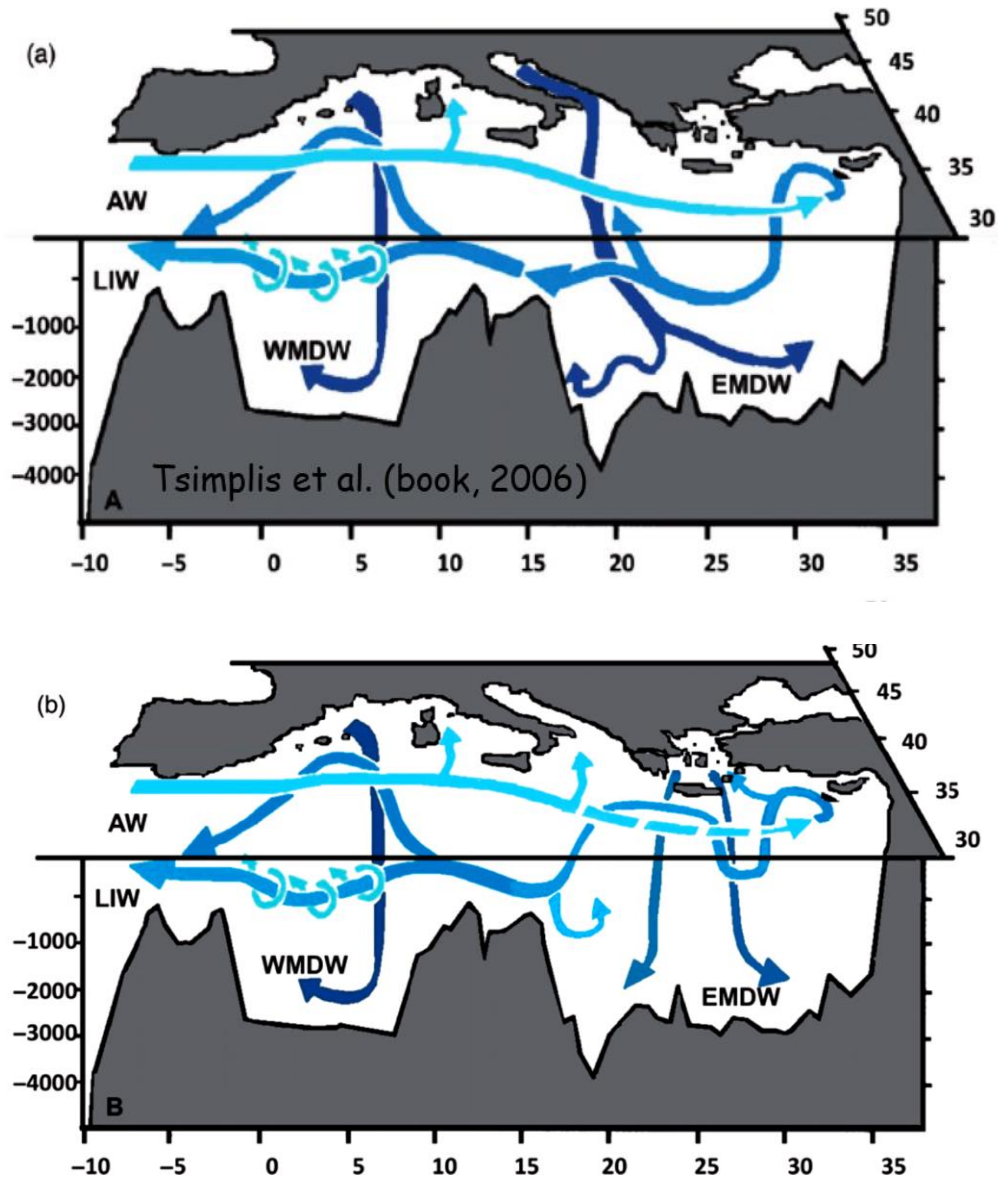


Figure 3. Schematic graph of the bathymetry and main water masses in the MedSea before EMT (a) and during EMT (b). The light blue arrow represents the fresher surface Atlantic Water (AW) entering through the Strait of Gibraltar to the Western basin, and all the way to the Eastern basin. It then becomes denser, and flows back to the Atlantic as Levantine Intermediate Water (LIW), represented by a darker blue arrow. Denser water outflows from the Adriatic Sea, conforming the East-Mediterranean Deep Water (EMDW), and from the Western-Mediterranean Deep Water (WMDW), both represented by even darker blue arrows.

represented in a pre-EMT (a) and during EMT (b) conditions.¹³

1.3. Why CO₂ in the Mediterranean Sea

The MedSea is considered by some authors¹⁴ as an ocean in miniature in which many internal processes take place as they do in the world wide ocean.¹⁴ They consider it as a “basin laboratory” because these processes may be more easily detected, studied and monitored. This fact makes its study interesting not only to know the MedSea better itself, but also all oceans behavior.

Another interesting characteristic of the MedSea is its ability to capture large amounts of anthropogenic carbon dioxide (C_{ant}), which is the CO₂ generated from human activities. Such capacity is given by the high alkalinity and temperature of the surface waters, which can be rapidly transported to deeper sections¹⁵, allowing the sequestration of more CO₂ in the surface.

The reservoirs of C_{ant} in the MedSea are one of the highest of the global ocean as it can be observed in **Figure 4**¹⁶, meaning that an important amount of the world's anthropogenic emissions of CO₂ are stored in the MedSea despite its relatively small volume.¹⁵

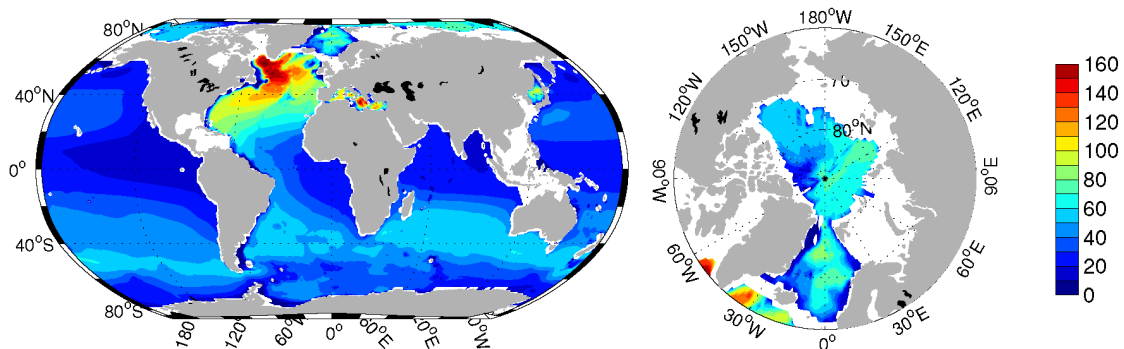


Figure 4. Representation of the oceanwide distribution of C_{ant} from Lee et al., 2011. Scale in $\text{mol}\cdot\text{m}^{-2}$. As it can be observed, the higher concentrations are found in the North Atlantic Ocean and in the MedSea.

Also, as it was pointed out in section 1.2, the MedSea is surrounded by many countries, and therefore, regional climate, fisheries and tourism are important areas interested in the better knowledge of this sea.

1.4. Med-SHIP program

Despite all the mentioned facts that make the MedSea an interesting target for scientists, up until 2011 it was only sampled by national expeditions in regional areas. Large international programs have been disregarding it, such as the World Ocean Circulation Experiment (WOCE) and its repetition, both coordinated by the Global Ocean Ship-Based Hydrographic Investigation Program (GO-SHIP).¹⁷

The creation of the Med-SHIP program fills this gap to collect hydrographic observations in the MedSea with two main objectives: “(1) to observe and quantify long-term changes in marine physical and biogeochemical properties in the Mediterranean Sea, where the shorter turnover time scale suggest they can be extrapolated to the global ocean, and (2) to observe changes in thermohaline circulation and to determine how often and how much deep water is formed, and whether the currents are changing in position and intensity.”¹⁷

In 2011 three oceanographic cruises were conducted coordinately, with slightly different scopes, but allowing for a general view of the properties and distribution of the studied parameters along the major sub-basins. These cruises⁽ⁱⁱ⁾ were the German R/V *Meteor* (cruise M84/3, Istanbul to Vigo, 5-28 April 2011), the German R/V *Poseidon* (cruise POS414, Genoa to messina, 31 May to 13 June 2011) and the Italian R/V *Urania* (cruise EF11, Bari to La Spezia, 22 April to 2 May 2011).¹⁴

MSM72

To obtain actualized information on the MedSea, and to monitor its evolution comparing it with that provided by past cruises, the cruise MSM72 was organized inside the MED-Ship effort. The German R/V *Maria S. Merian*, departed from Crete on the 1st of March 2018 and arrived in Cádiz on the 4th of April 2018, intending to follow the route indicated in Figure 5.

Unluckily, due to political issues, the stations planned for the Levantine basin could not be sampled and the station plan had to be changed continuously in order to adjust to the schedule and situation, however the lack of stations in the Levantine basin was compensated with more stations in the rest of the cruise.

⁽ⁱⁱ⁾ R/V stands for Research Vessel. In italics the vessel's name. In parenthesis the name of the cruise (using an acronym of the vessel and the number of cruise), the origin and destiny and the dates when it took place.

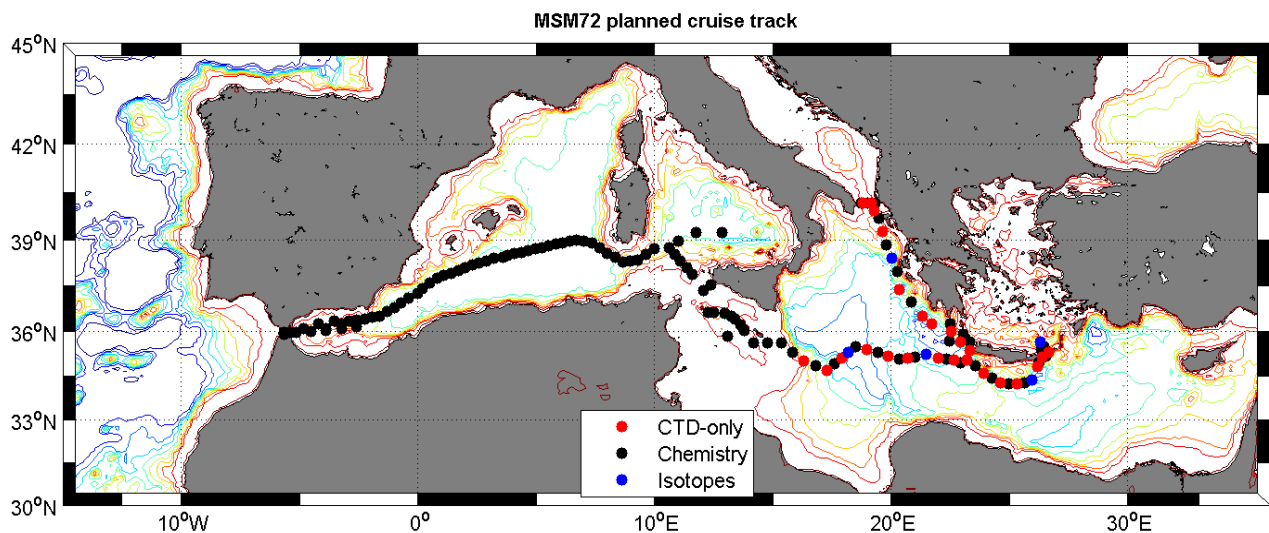


Figure 5. Map of stations planned for the MSM72 at the beginning of the cruise. As the legend reads, red dots correspond to physical stations, where only CTD measurements were carried. The black dots correspond to chemistry stations, that is, all variables were sampled except for isotopes and POC/PON, which are sampled only in Isotope stations, represented by blue dots. Map made by T. Tanhua.

There were seven international research groups onboard, dedicated to physical oceanography, chemical oceanography and marine ecology, working in an interdisciplinary-coordinated way. From Germany, the *University of Hamburg* and GEOMAR; from Italy, the *Istituto Nazionale di Oceanografia e di Geofisica Sperimentale (OGS)*, the *CNR Istituto di Biofisica Unità Operativa di Pisa (CNR-P)* and the *Istituto di Scienze Marine (ISMAR)*; from Greece, the *Hellenic Centre for Marine Research (HCMR)*; from Lebanon, the *National Council for Scientific Research in Lebanon (CNRS-L)*; and from Spain, the *Instituto Español de Oceanografía (IEO) - Centro Oceanográfico de A Coruña*.

The group in charge of the carbonate system sampling and measuring was formed by Dr. Noelia M. Fajar and Dr. Elisa F. Guallart (IEO), Dr. Abed El Rahman Hassoun from the CNRS-L and myself.

Figure 6. German research vessel *Maria S. Merian* in which the cruise MSM72 took place.



OBJECTIVES OF TFG

Participation in the MSM72 oceanographic cruise in March-April 2018, as part of the IEO group responsible of CO₂ measurements in the water column; pH, alkalinity, total inorganic carbon and carbonate ion. It will be a campaign on board of the German ship "RV Maria S. Merian", departing from Crete, and finishing in Cadiz. Apart from onboard analysis, student will treat the pH raw data to finally remit the final campaign report. The TFG will consist on presenting and describing these data, to study biogeochemical properties of the different water masses in the Mediterranean sea, from the Ionian basin to the gulf of Cadiz.

Participación en la campaña oceanográfica MSM72 en Marzo-Abril de 2018, como parte del grupo del IEO responsable de las medidas de CO₂ en la columna de agua; pH alcalinidad, carbono inorgánico total e ión carbonato. La campaña será a bordo del buque alemán "RV Maria S. Merian", saliendo de Creta y atracando en Cádiz. Además de los análisis a bordo, se tratarán los datos brutos de pH para remitir el informe final de la campaña. El TFG consistirá en la presentación y descripción de estos datos, así como el estudio de las diferentes masas de agua en el mar Mediterráneo, desde el mar Jónico hasta el golfo de Cádiz.

Participación na campaña oceanográfica MSM72 en Marzo-Abril do 2018, como parte do grupo do IEO responsable das medidas de CO₂ na columna de auga; pH, alcalinidade, carbono inorgánico total e ión carbonato. A campaña será a bordo do "RV Maria S. Merian", saíndo de Creta e chegando a Cádiz. Ademais dos análises a bordo, a estudante tratou os datos brutos de pH co fin de remitir o informe final da campaña. Este TFG consiste na presentación e descripción destes datos, así como o estudo das diferentes masas de auga no mar Mediterráneo, dende mar Jónico ata o golfo de Cádiz.

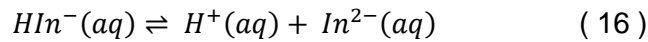
METHODOLOGICAL FUNDAMENTALS

3.1. Determination of $[H^+]$ concentration

Fundamentals of spectrophotometric determination of pH

The pH values were determined by the spectrophotometric method described by Clayton and Byrne¹⁸. This method consists on adding *m*-cresol purple (m-CP) as indicator dye to the water sample and measuring the absorbance. This m-CP indicator is a sulphonephtalein indicator, which are the most appropriate for surface-to-deep pH profiles in the ocean.

The indicator loses protons in two consecutive dissociation reactions. The pK_{H_2In} of the first deprotonation is around 2. For the second one, pK_{HIn} is close to 8. Seawater samples have a pH close to this second pK_{HIn} , and therefore derivation of the pH equation will be focused on this dissociation reaction.



In^{2-} stands for the fully deprotonated form of the indicator (purple) and HIn^- for the single protonated form (yellow)¹⁹. As it was mentioned in section 1.1, seawater standard state is defined to have an activity coefficient equal to one, and therefore activities may be substituted by concentrations. The equilibrium constant is defined as

$$K_{HIn} = \frac{[In^{2-}][H^+]}{[HIn^-]} \quad (17)$$

Taking logarithms,

$$\log K_{HIn} = \log \left(\frac{[In^{2-}][H^+]}{[HIn^-]} \right) = \log \left(\frac{[In^{2-}]}{[HIn^-]} \right) + \log [H^+] \quad (18)$$

Rearranging and changing the sign

$$-\log K_{HIn} = -\log \frac{[I^{2-}]}{[HIn^-]} - \log [H^+] \quad (19)$$

the Henderson-Hasselbach equation for a buffer solution may be obtained, to calculate the pH values

$$pH = pK_{HIn^-} + \log \frac{[I^{2-}]}{[HIn^-]} \quad (20)$$

A relation between $[I^{2-}]$ and $[HIn^-]$ may be estimated by spectrophotometric measurements applying the Lambert-Beer law.

$$\frac{A_{\lambda}}{l} = \varepsilon_{\lambda}^{HI n^{-}} \cdot [HI n^{-}] + \varepsilon_{\lambda}^{In^{2-}} \cdot [In^{2-}] + B_{\lambda} + e \quad (21)$$

Where ε_{λ}^i are the corresponding molar extinction coefficients at a wavelength λ , B_{λ} is the background absorbance of the sample and e the error related to instrumental noise. l is the pathlength of the cell.

B_{λ} may be subtracted doing a baseline for each sample at the wavelengths of interest before measuring and the term e may be neglected assuming no instrumental error.

If absorbance measurements are carried out at two different wavelengths, the ratio between the concentrations of both species may be obtained.

In order to achieve higher precision, the selection of these two wavelengths is important. The maximum of absorbance of each species is the optimal choice, because in that section of the spectrum, small variations of the wavelength will result in minimal variations of the recorded absorbance. The following graph (**Figure 7**)¹ shows the spectra for acid and basic forms of the indicator used, m-cresol purple.

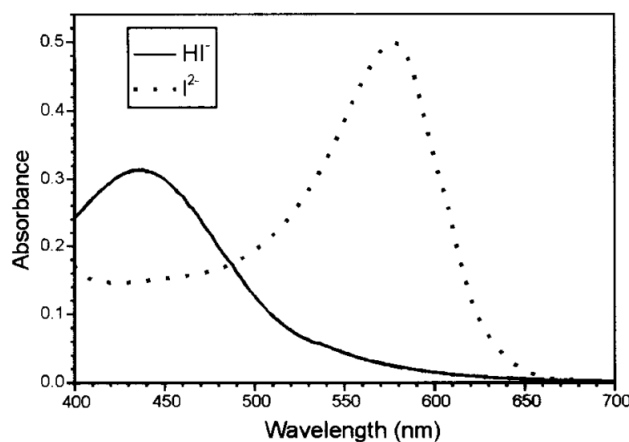


Figure 7. Absorbance spectra for both species $HI n^{-}$ and In^{2-} of m-cresol purple. Maxima are observed at 434 nm for the single protonated –more acid- form ($HI n^{-}$) and at 578 nm for the fully deprotonated–more basic- one (In^{2-}).¹ The point where both graph cross over each other is the isobestic point, at 486 nm.

The Lambert-Beer law could be expressed as follows

$$\frac{A_{\lambda_1}}{l} = \varepsilon_{\lambda_1}^{HI n^{-}} \cdot [HI n^{-}] + \varepsilon_{\lambda_1}^{In^{2-}} \cdot [In^{2-}] \quad ; \quad \frac{A_{\lambda_2}}{l} = \varepsilon_{\lambda_2}^{HI n^{-}} \cdot [HI n^{-}] + \varepsilon_{\lambda_2}^{In^{2-}} \cdot [In^{2-}] \quad (22) \text{ (23)}$$

Dividing both expressions (22) and (23) by $[HI n^{-}]$

$$\frac{A_{\lambda_2}}{l \cdot [HI n^-]} = \varepsilon_{\lambda_2}^{HI n^-} + \varepsilon_{\lambda_2}^{In^{2-}} \cdot \frac{[In^{2-}]}{[HI n^-]} \rightarrow \frac{[In^{2-}]}{[HI n^-]} = \left(\frac{A_{\lambda_2}}{l \cdot [HI n^-]} - \varepsilon_{\lambda_2}^{HI n^-} \right) \cdot \frac{1}{\varepsilon_{\lambda_2}^{In^{2-}}} \quad (24)$$

$$\frac{A_{\lambda_1}}{l \cdot [HI n^-]} = \varepsilon_{\lambda_1}^{HI n^-} + \varepsilon_{\lambda_1}^{In^{2-}} \cdot \frac{[In^{2-}]}{[HI n^-]} \rightarrow [HI n^-] = \frac{A_{\lambda_1}}{l \cdot \left(\varepsilon_{\lambda_1}^{In^{2-}} \cdot \frac{[In^{2-}]}{[HI n^-]} + \varepsilon_{\lambda_1}^{HI n^-} \right)} \quad (25)$$

Substituting expression (25) into (24).

$$\frac{[In^{2-}]}{[HI n^-]} = \left[\frac{A_{\lambda_2}}{A_{\lambda_1}} \left(\varepsilon_{\lambda_1}^{In^{2-}} \cdot \frac{[In^{2-}]}{[HI n^-]} + \varepsilon_{\lambda_1}^{HI n^-} \right) - \varepsilon_{\lambda_2}^{HI n^-} \right] \cdot \frac{1}{\varepsilon_{\lambda_2}^{In^{2-}}} \quad (26)$$

Rearranging again:

$$\frac{[In^{2-}]}{[HI n^-]} = \frac{\frac{A_{\lambda_2}}{A_{\lambda_1}} \cdot \frac{\varepsilon_{\lambda_2}^{HI n^-}}{\varepsilon_{\lambda_1}^{HI n^-}}}{\frac{\varepsilon_{\lambda_2}^{In^{2-}}}{\varepsilon_{\lambda_1}^{HI n^-}} - \frac{A_{\lambda_2}}{A_{\lambda_1}} \cdot \frac{\varepsilon_{\lambda_1}^{In^{2-}}}{\varepsilon_{\lambda_1}^{HI n^-}}} \quad (27)$$

And the substitution of the following absorbance and extinction coefficient ratios

$$R = \frac{A_{\lambda_2}}{A_{\lambda_1}} \quad e_1 = \frac{\varepsilon_{\lambda_2}^{HI n^-}}{\varepsilon_{\lambda_1}^{HI n^-}} \quad e_2 = \frac{\varepsilon_{\lambda_2}^{In^{2-}}}{\varepsilon_{\lambda_1}^{HI n^-}} \quad e_3 = \frac{\varepsilon_{\lambda_1}^{In^{2-}}}{\varepsilon_{\lambda_1}^{HI n^-}} \quad (28)$$

leads to the expression²

$$pH_T = pK_{HI n^-} + \log \left(\frac{R - e_1}{e_2 - R \cdot e_3} \right) \quad (29)$$

The dimensionless extinction coefficient ratios have been measured³ for species $HI n^-$ and I^{2-} at wavelengths $\lambda_1 = 434$ nm and $\lambda_2 = 578$ nm, obtaining the values in **¡Error! No se encuentra el origen de la referencia.**²⁰

Constant	Empirical value
e1	$6.91 \cdot 10^{-3}$
e2	2.2220
e3	0.1331

Table 2. Extinction coefficient ratios for *m*-cresol Purple for wavelegths 434 and 758 nm.

The equilibrium constant $K_{HI n^-}$ depends on salinity and temperature, and $pK_{HI n^-}$ has been determined for *m*-cresol purple as:³

$$pK_{HI n^-} = \frac{1245.69}{T(K)} + 3.8275 + 0.00211(35 - S) \quad (30)$$

Where $293\text{ K} \leq T \leq 303\text{ K}$ and $30 \leq S \leq 37$

Finally, the expression to calculate pH values using the total hydrogen concentration scale²

$$pH_T = \frac{1245.69}{T(K)} + 3.8275 + 0.00211(35 - S) + \log\left(\frac{R - 6.91 \cdot 10^{-3}}{2.2220 - R \cdot 0.1331}\right) \quad (31)$$

Where T is the temperature in Kelvin, S is the salinity and R the ratio between absorbance at the selected wavelengths.

The precision of this method was assessed as 0.0004 and the assigned accuracy was 0.001 pH units.¹⁸

ΔR Correction

The addition of indicator perturbs slightly the real pH of the sample, since the dye has some acid-base properties itself.

This perturbation depends on the acidity difference between seawater and indicator. It is minimized by the adjustment of the dye solution pH, therefore, the empirical evaluation of the correction should be performed for each batch of indicator solution. In order to do so, a second addition of dye may be made to a series of seawater samples with different pH. The absorbance ratio R is determined for both additions (R_1 and R_2) and the variation between the ratios obtained for first and the second addition ($\Delta R = R_2 - R_1$) per mL of added dye is represented against the ratio obtained for the first addition. Applying the least-squares method, a linear regression is obtained³

$$\frac{\Delta R}{V} = A + BR_1 \quad (32)$$

The corrected R that will be used in equation (31) to obtain the final pH value will be calculated as

$$R = R_1 + (A + BR_1)V \quad (33)$$

3.2. TA determination in seawater

Total alkalinity (TA) was measured by a potentiometric method. The titration was carried out with hydrochloric acid 0.1 N. Classical methods use computerized systems which determine the end point of the titration curve in around 30 minutes.³ Pérez et al. proposed an improved method which only takes 3-4 minutes per sample, using a 4.4 buffer solution to calibrate the electrode.

For calculations, the alkalinity definition neglects smaller concentration terms in equation (10) to:

$$A_T = [HCO_3^-] + 2[CO_3^{2-}] + [B(OH)_4^-] - [H^+]_F + [OH^-] \quad (34)$$

At the equivalence point, the alkalinity of a sample equals the concentration of titrant (HCl) times the volume used to reach the end point, divided by the volume of the sample.

$$A_T = \frac{[HCl] \cdot V_{HCl}}{V_{sample}} \quad (35)$$

The final expression for the determination of total alkalinity is obtained after substitution of several terms calculated by several authors²¹ into equation (35), but it won't be reflected in this work because it is all computerized and the deduction is beyond the scope of this thesis.

TA precision was defined as the reproducibility from certified reference material (CRM) analyses (<1 $\mu\text{mol}/\text{kg}$) and the accuracy is within 2 $\mu\text{mol}/\text{kg}$.²²

3.3. DIC determination in seawater

DIC is determined following a coulombimetric titration. A known amount of sea water sample, 20 mL in this case, is dispensed into a stripping chamber. There, it is acidified with H_3PO_4 to have all the present carbon (carbonate, bicarbonate and carbon dioxide) as CO_2 (see equations (12) and (13)) . A carrier inert gas transfers the generated CO_2 gas into a titration cell where it is trapped by ethanolamine.³

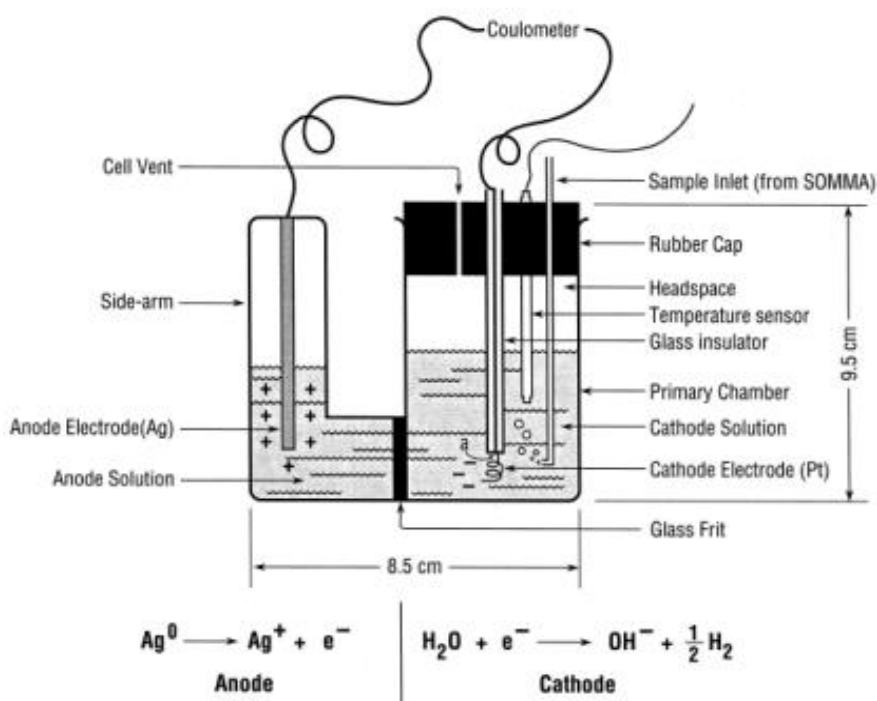
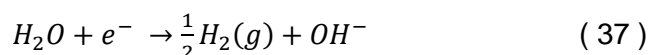


Figure 8. Scheme of a titration cell for the SOMMA, the antecedent of the used device, the VINDTA. The cell is anyway equal for both systems.

The hydroxyethylcarbamic acid that is formed is coulometrically titrated with hydroxide ions generated by the electrolysis of water taking place at the cathode,



while at the anode, silver dissolves as silver cation



The coulometer measures the amount of electrical charge between anode and cathode, and generates electrical pulses or counts. To obtain the concentration of inorganic carbon, the data about the end point of the titration given by the VINDTA system in counts per minute, is transformed to moles per kg following these calculations:

First, the amount of inorganic carbon in the sample is calculated²³:

$$\mu\text{mol } C_{exp} = (\text{Counts} - \text{Blank} \cdot RT) \cdot \frac{1 \mu\text{mol } C}{4.82445 \cdot 10^3 \text{ counts}} \quad (39)$$

This experimentally obtained amount of carbon is transformed into concentration dividing it over the mass of the sample, m_s .

$$DIC_{exp} (\mu\text{mol}/\text{kg}) = \frac{\mu\text{mol } C_{exp}}{m_s} \quad (40)$$

A correction term caled the CALFACTOR is added to the calculations because there is a deviation²³ from the known as real value due to loss of carbon during extraction or titration. The CALFACTOR may be calculated as the ratio of the given theoretical CRM concentration and the experimentally obtained one.

$$CALFACTOR = \frac{DIC_{th}}{DIC_{exp}} \quad (41)$$

The precision of DIC method is 1 $\mu\text{mol}/\text{kg}$ and the accuracy is 2 $\mu\text{mol}/\text{kg}$.²³

3.4. Determination of CO_3^{2-}

Carbonate ion, is directly determined by a spectrophotometrical analysis, in a way very similar to the already explained pH method (section 3.1, page 25) but using a lead complexing agent, $\text{Pb}(\text{ClO}_4)_2$ or PbCl_2 , to form a lead carbonate complex which absorbs in the UV region.

In this case the chosen wavelengths are 250 and 234 nm. Following a deduction analogous to that for pH, the final equation to calculate carbonate ion concentration in seawater is: ⁶

$$-\log[\text{CO}_3^{2-}]_T = \log\left(\frac{\text{CO}_3\beta_1}{e_2}\right) + \log\left(\frac{R-e_1}{1-R\frac{e_3}{e_2}}\right) \quad (42)$$

Where the coefficients R, e_1 , e_2 and e_3 are

$$R = \frac{A_{\lambda 250}}{A_{\lambda 234}} \quad e_1 = \frac{\epsilon_{\lambda 250}^{\text{PbCO}_3}}{\epsilon_{\lambda 234}^{\text{PbCO}_3}} \quad e_2 = \frac{\epsilon_{\lambda 250}^{\text{Pb}}}{\epsilon_{\lambda 234}^{\text{PbCO}_3}} \quad e_3 = \frac{\epsilon_{\lambda 234}^{\text{Pb}}}{\epsilon_{\lambda 250}^{\text{Pb}}} \quad (43)$$

The salinity-dependent stability constant for the formation of the lead carbonate complex, PbCO_3^0 is given as:

$$\text{CO}_3\beta_1 = \frac{[\text{PbCO}_3^0]}{[\text{Pb}^{2+}]_T[\text{CO}_3^{2-}]_T} \quad (44)$$

The relative errors are $\pm 5.8 \mu\text{mol}\cdot\text{kg}^{-1}$ when $[\text{CO}_3^{2-}] = 250 \mu\text{mol}/\text{kg}$.²⁴

WORK MADE AT SEA

4.1. Organization

In this oceanographic cruise, as there were several groups working in the areas of chemical oceanography, physical oceanography and medium biology, the demand for seawater in some stations and depths was important.

The water was taken using a rosette (Figure 9. Rosette on the deck. Each Niskin bottle can contain 10 L. It is thrown to the sea by members of the physics group in coordination with the crew. In the bottom part, the yellow CTD may be observed. Figure 9), a metal cylindrical structure holding twenty-four 10 L Niskin sampling bottles, which have to be open when the rosette is launched into the water to avoid implosion. The rosette also carried a CTD device (Conductivity, Temperature and Depth), which provides values for salinity, temperature and pressure as the rosette goes down. That way, scientists can choose which depth may be more interesting to sample, and so the rosette is stopped on its way up at the decided depths to close as many bottles as seawater demand requires.

At a given station, each Niskin bottle (numerated from 1 to 24) corresponded to one depth, so the collection of samples for several parameters was simpler and organized.

As samples are drawn, a headspace is created in the Niskin sampling bottle, leading to

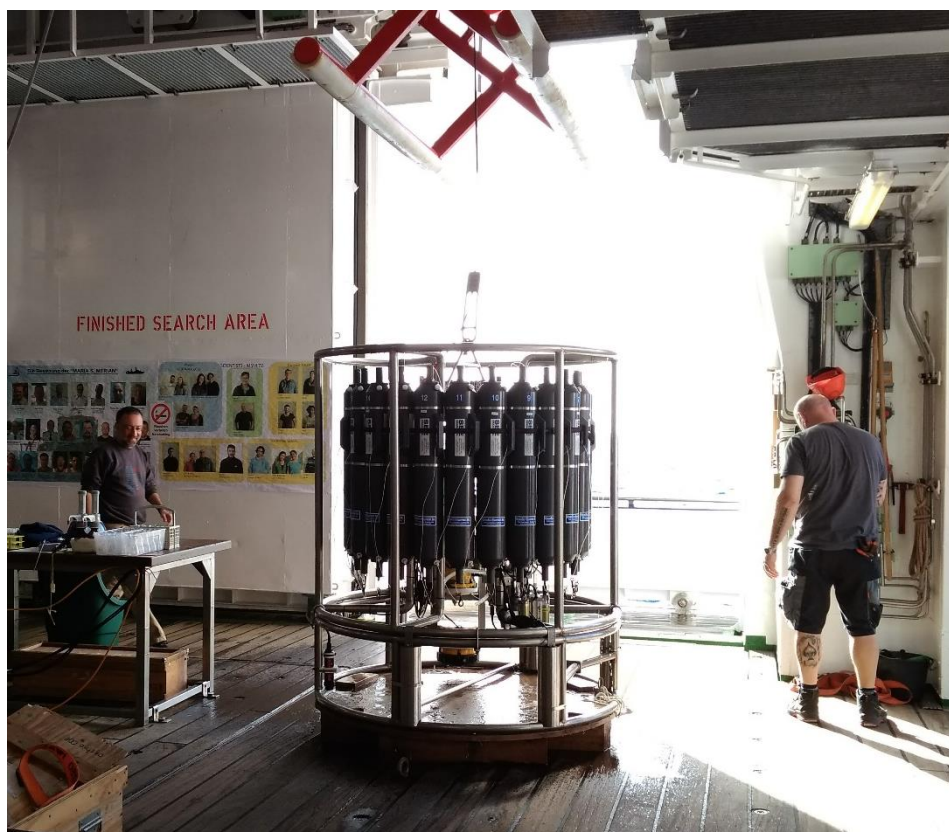


Figure 9. Rosette on the deck. Each Niskin bottle can contain 10 L. It is thrown to the sea by members of the physics group in coordination with the crew. In the bottom part, the yellow CTD may be observed.

the consequent gas exchange between water and air. Some parameters such as pH or DIC are affected by this exchange and should be drawn first.

The immediate conclusion was to establish a well-organized sampling hierarchy: tracers, O₂, DIC, pH, DOC and OM, CO₃²⁻, TA and finally nutrients.

A table with all parameters and depths was hung in the sampling area so that the right order was followed.

The four parameters sampled by the CO₂ system team (DIC, pH, TA and CO₃²⁻) were drawn attaching an approximately 20 cm silicon sampling tube to the Niskin bottle. Further detail on each technique will be presented along this section.

The number of samples collected at each station for each parameter is reflected in Table 14.

4.2. pH measurements

Sampling

Samples were collected in cylindrical optical glass Hellma cells of 28 mL volume and 10 cm of path-length. Water was overflowed until no air bubbles were observed, and cells were sealed using two PTFE caps.

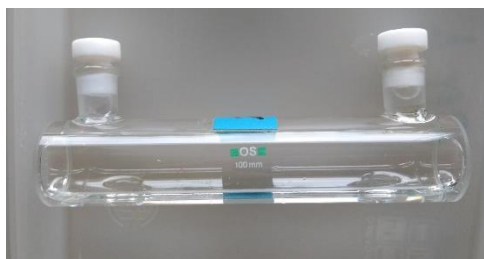


Figure 10. Cylindrical cuvettes for pH determinations. Made of quartz they can also be used for carbonate ion determinations. On the right, the range of colours of *m*-CP from the single protonated form to the fully deprotonated species.

Analysis procedure and equipment

Cells with samples were stored in an incubator at 25°C warmed by a thermostatic bath for around one hour before the analysis. Absorbance was determined using a Shimadzu UV-2600 double beam spectrophotometer, and the corresponding software, UV Probe. The temperature of all measurements was controlled with a JULABO F12 ED (12L) thermostatic bath. Figure 11 is a picture of the equipment as it was set in the on-board laboratory.



Figure 11. Spectrophotometer on the right, the wooden box is the incubator and above it, the cells for pH measurements as they were set up in the Trokenlabor at the R/V Maria S. Merian. Photo taken by N. Fajar.

The indicator used was m-cresol purple (Sigma Aldrich), prepared in seawater (2mM) and kept in the dark, with no air contact

The absorbance of the cell and the sample were recorded from 400 to 750 nm in order to set a baseline. This range of wavelengths includes both maxima for acid and basic forms of the dye ($\lambda_1=434$ and $\lambda_2=578$ nm respectively), a non-absorbing wavelength as a control of the method and procedure ($\lambda_3=730$ nm), and the isosbestic point (487.6 nm).

Then, 50 μ L of the dye m-cresol purple were added to the samples and the absorbance was measured three times at the four chosen wavelengths.

Quality control

First quality control

After each analysis, the obtained data were recorded in one excel file where the absorbance ratio, R for each of the three measurements were calculated as $R = \frac{\lambda_2 - \lambda_3}{\lambda_1 - \lambda_3}$, along with average and corresponding standard deviation per sample.

Before calculating pH values, raw data as processed and cleaned. A code was assigned to each sample applying the formula

$$Code = Station \cdot 1000 + Cast \cdot 100 + Niskin \quad (45)$$

Formula used to assign a unique code to each sample. If a sample was taken from Niskin 15, from the second cast at station 44, its corresponding code would be 44217.

To make the cleaning easier to understand, a code of numbers was established assigning a flag number to certain possible types of error, as given in Table 3.

Flag Number	Meaning
Flag 2	OK
Flag 3	Outlier in graphic representation. Probably wrong
Flag 4	Known to be bad from lab notebook/wrong blank
Flag 6	Replicate
Flag 9	Not sampled

Table 3. Flag numbers associated to different types of errors used in the processing of pH data.

First, absorbance values at 730 nm were checked since it is a non-absorbing wavelength used as a control for human error, they are represented in Figure 12. The R corresponding to absorbance values greater than 0.009 were eliminated, and if the three replicates were greater, that sample was marked as a flag 4.

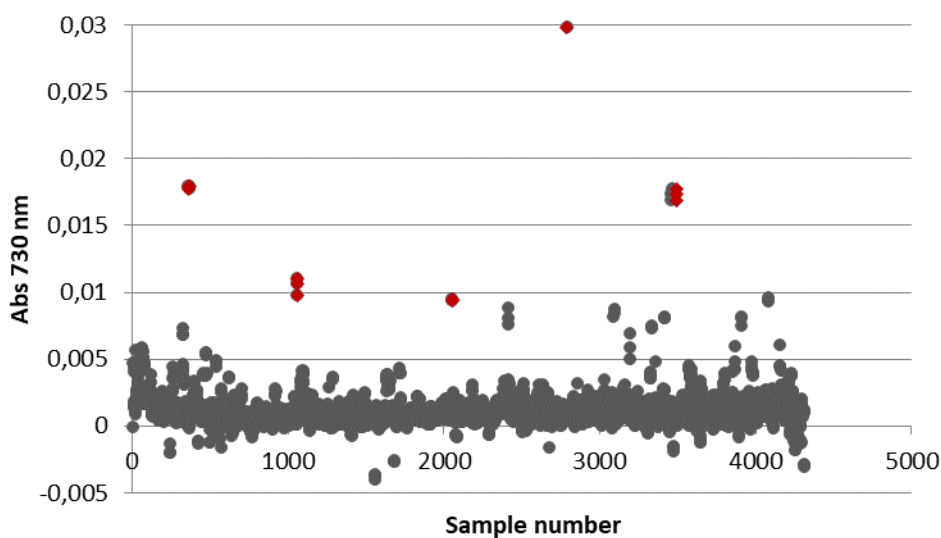


Figure 12. Absorbance values recorded at 730 nm of all analyzed samples. In red the eliminated dots, higher than 0.009.

Then, STD (R), standard deviation of the R, values were looked at. Standard deviations greater than 0.05 were marked and the corresponding R values eliminated. The STD (R) was evaluated when (a) only the first R value was eliminated and if STD (R) was still greater than 0.05, (b) only the third was eliminated. If neither (a) nor (b) caused a big enough decrease in the STD (R), only the third value was kept. Note that every time an R value was eliminated, the average of absorbance and corresponding STD at the isosbestic wavelength (478.6 nm) was recalculated.

Finally, absorbance at the isosbestic wavelength was reviewed. The average absorbance for an addition of 50 μ L is 0.25. Greater values indicate that either too much dye was added, or that a second addition was performed in order to make the ΔR correction (explained with detail in section 3.1, page 25). Lower values imply a too low addition of dye.

Duplicates were also examined so that the code is assigned to the right measurement. All this cleaning process was followed with the lab notebook and the sampling sheet, so any irregularity in the sampling or during the analysis was taken into account.

Accuracy

In order to measure the accuracy of pH measurements, samples of TRIS buffer certified seawater distributed by A.G. Dickson from the Scripps Institution of Oceanography were analyzed during the cruise MSM72. The measurements were performed at three different temperatures, so that both Eastern and Western basins pH values would be covered. The average of the obtained pH values is shown in Table 4 with standard deviations and number of measured samples.

T^a (°C)	pH	STD	n
25	8.0981	0.0009	4
27	8.0365	0.0014	5
29.7	7.9579	0.0024	5

Table 4. Mean temperature and pH measured with respective standard deviation (STD) and number of samples analyzed (n).

Precision

A typical reproducibility analysis was performed on each basin. For that, the pH of four or five samples taken from the same Niskin bottle were analyzed. Obtained results are given in Table 5.

Basin	St	Salinity	Depth (m)	pH	STD	n
Western	52	38.727	3402.37	7.9590	0.0003	6
	56	38.605	103.56	7.9737	0.0005	5
Eastern	100	38.491	2764.03	7.8975	0.0004	4
	102	38.045	104.75	7.9357	0.0009	4

Table 5. Characteristics of seawater samples used for the precision analysis. Average calculated pH, along with standard deviations (STD) and number of samples collected from each Niskin (n).

4.3. TA measurements

Sampling

TA samples were taken in 600 mL borosilicate bottles. First, the sample bottle and cap were rinsed, then bottles were filled smoothly, placing the end of the drawing tube at the bottom. Water was allowed to overflow by one time the volume of the flask and immediately sealed.



Figure 13. Box for transporting TA sample bottles from laboratory to sampling area and viceversa.

Analysis procedure and equipment

Samples were stored and allowed to temper in the laboratory for no longer than two days. An exact volume of the sample was taken using a Knudsen pipette²⁵ (Figure 14) of 186 mL and poured into a 220 mL Erlenmeyer flask. Titration is carried out using an automatic potentiometric titrator *Titrande 904 Metrohm*, with a *Metrohm Aquatrode Plus* combination glass electrode and a *Pt-1000 probe* to check the temperature. The system is coupled with a 10 mL

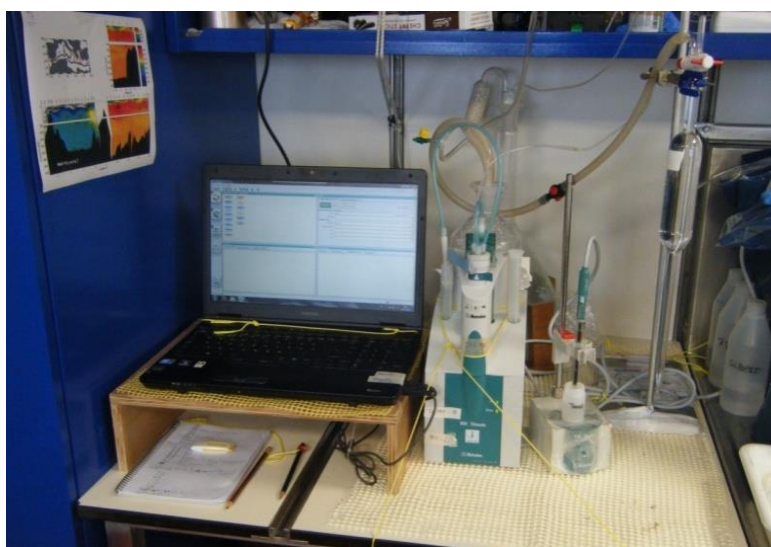


Figure 14. Equipment for TA determinations. On the computer's right in order, *Titrande 904*, *stirrer 801 (Metrohm)* and *knudsen pipette* attached to an air pump. On the right, schematic *Knudsen pipette*, which allows quick and accurate transfer of a constant volume of liquid (sea water). A double sided vent (C) allows for either the establishment of a flow between the body of the pipette and one of the branches (A or B) or the isolation of the body from both branches.

burette or exchangeable unit.

The titrant was hydrochloric acid 0.1 N, usually prepared by diluting a 0.5 mol/L of commercial HCl, supplied by Riedel-deHaën® (Fixanal 38285) with distilled water into a graduated 5 L flask at controlled temperature conditions. However, on this cruise, the available reagent onboard was Titrisol® Hydrochloric acid 1 N, to be diluted in 1 L. The limited availability of material lead to the preparation of 5 L of HCl (0.2 N), which was then diluted to 0.1 N using two graduated flasks of 500 mL and 1 L. As the titrants needs to be of a known exact concentration, around 500 mL of each of the two batches prepared during the cruise were stored to be titrated at the IEO laboratory in A Coruña.

[Na₂CO₃] (mol/L)	v HCl (mL)	[HCl] (mol/L) t(95%, n=5)	Confidence interval t(95%, n=5)
1.111	100	0.0996 ± 0.0003	0.099 mol/L-0.100 mol/L

Table 6. Data from titration of HCl with sodium carbonate.

The corresponding titrations were performed by the automatic titrator used for alkalinity measurements, but using Na₂CO₃ as titrant this time. The final HCl concentrations for each batch are observed in

Table 6.

The sequence for each analysis session or batch included the analysis of some standards and duplicates to check it was repeating properly.

Step	Procedure
Buffer & calibration	~30 min with new phthalate buffer and calibration of electrode
Prepare	Titrant is released to eliminate air bubbles in the tubes
777	Seawater from the tap is titrated to start the system*
888	Substandard is analyzed to control drift along station and cruise*
999	CRM is analyzed to check the accuracy of the system*
St 1	First station is analyzed
888	Substandard is analyzed to control drift along station and cruise *
St 2	Next stations are analyzed, a substandard is analyzed in between stations
888	Substandard is analyzed to control drift along station and cruise *
Close	Electrode is left submerged in left over buffer

Table 7. Order of an alkalinity session of analysis. Replicates are conducted in steps in italics and marked with * in the procedure. If difference between replicates was greater than 1 $\mu\text{mol/kg}$, a third measurement was performed. If it was smaller, analysis continued to the next step.

Quality control

Accuracy

To control the accuracy of TA measurements, a CRM was analyzed at the beginning of each analysis. The obtained TA values for each batch of CRM are reflected in ¡Error! No se encuentra el origen de la referencia., where the gray squares are the measured TA values and the circles represent the mean value with the corresponding error bar per analysis session. The horizontal dashed lines are the mean standard deviation for the twelve batches of analysis.

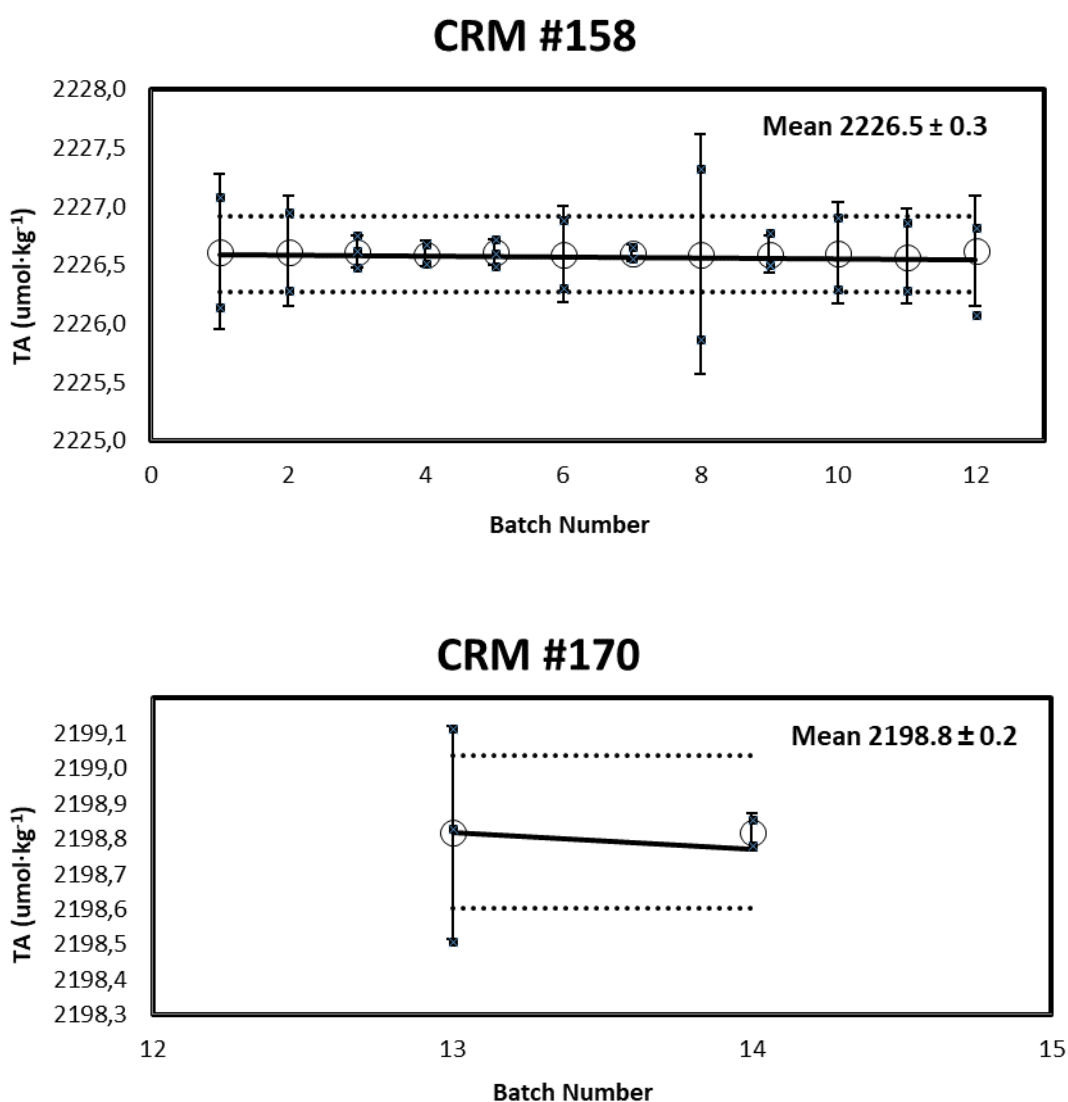


Figure 15. Alkalinity measurements of CRM analyzed during the cruise represented versus the session number. Batch #158 (sessions 1-12) and batch #170 (sessions 13-14). Plots by N. Fajar.

An extra calibration was conducted during the cruise MSM72 which consisted on the analysis of substandard seawater before and after each series of samples. The substandard was collected at the beginning of the cruise from the depth with the salinity minimum, at 700 m depth, in a 30 L container at least one day before its use. It was stored in the dark.

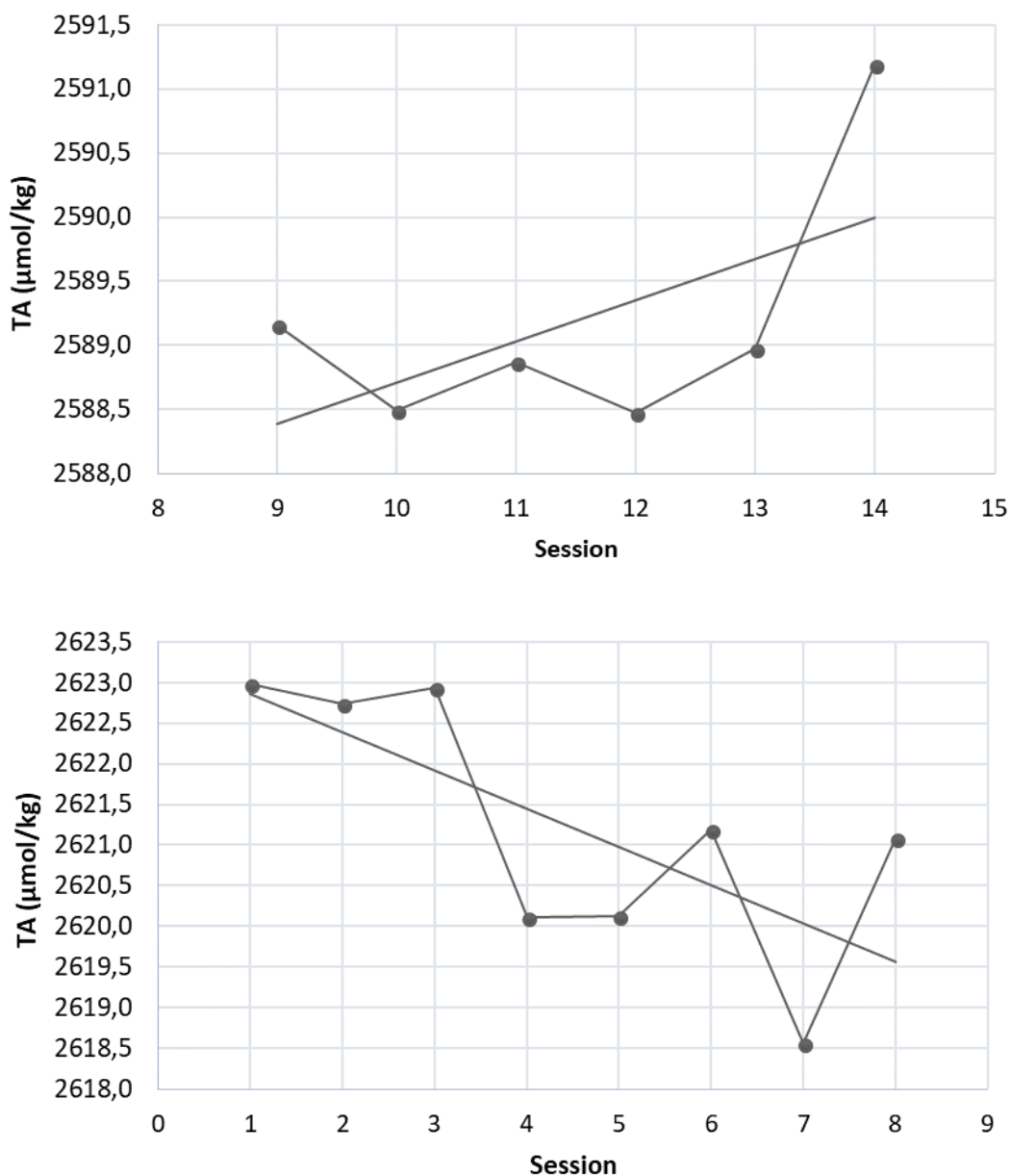


Figure 16. Representation of the mean TA for the substandard seawater versus the session number.

The objective of this substandard was to monitor the drift of TA determinations throughout the cruise. The values for this drift control are shown in **¡Error! No se**

encuentra el origen de la referencia. for the two different substandard used along MSM72.

In Table 8 a summary of both CRM and substandard quality control for TA analysis is given.

Session	Day 2018	Station	Δ pH	Fitted TA	Mean SUB TA	Av. Dif
1	4 March	1 2 4 8	0.01215	2 226.62±0.67	2 622.98±0.30	0.79 (47)
2	5 March	9 11 13	0.01315	2 226.62±0.47	2 622.73±0.42	0.68 (47)
3	7 March	17 20	0.0247	2 226.62±0.14	2 622.93±0.34	0.38 (28)
4	9 March	22 23 26	0.00495	2 226.60±0.11	2 620.11±0.91	0.56 (54)
5	13 March	30 32 34 38 40 42 43	0.0091	2 226.61±0.11	2 620.12±0.63	0.49 (82)
6	16 March	44 47 51 53	0.032	2 226.60±0.41	2 621.18±0.36	0.61 (85)
7	17 March	55 57 59 61 63	0.0348	2 226.61±0.07	2 618.56	0.55 (76)
8	21 March	66 68 70 72 73 75	0.0423	2 226.60±1.03	2 621.08±0.58	0.70 (77)
9	24 March	77 79 81 83 85 87 89	0.0421	2 226.60±0.16	2 589.16±0.47	0.57 (80)
10	26 March	91 93 95 97	0.0225	2 226.60±0.43	2 588.49±0.35	0.68 (72)
11	27 March	100 101 102 105	0.0125	2 226.58±0.40	2 588.87±0.19	0.69 (43)
12	29 March	109 111 113 115	0.0108	2 226.62±0.48	2 588.48±0.34	0.60 (67)
13	31 March	119 121 125 128	0.0115	2 198.82±0.30	2 588.98±0.27	0.55 (62)
14	1 April	130 132 134 136	0.0208	2 198.82±0.05	2 591.19±0.39	0.62 (38)

Table 8. Evaluation of the drift in the TA measurements by analysis of a CRM and substandards. All TA values in μ mol/kg

In Table 8, Δ pH is the pH correction applied to relate the TA determinations on the CRM to the corresponding nominal value for CRM batches #158 and #170 with a certified TA of $2227.85 \pm 0.54 \mu$ mol/kg and $2198.77 \pm 0.87 \mu$ mol/kg, respectively. The mean value of the TA measurements on the CRM samples is shown (Fitted TA \pm standard deviation). The mean value of the TA measurements on the substandard samples is also shown (Mean SUB TA \pm standard deviation). Av. Dif. and number of duplicates is the average of the difference in the duplicate's analyses.

Precision

The analysis of each sample was duplicated, one immediately after the other. The mean standard deviation for TA duplicates was 0.6 $\mu\text{mol/kg}$.

In the same way precision was evaluated for pH measurements, five samples drawn from the same Niskin bottle and TA average was determined. Table 5 shows obtained reproducibility values.

Basin	St	Salinity	Depth (m)	TA ($\mu\text{mol/kg}$)	STD	n
Western	52	38.727	3402.42	2610.93	0.65	5
	56	38.605	103.72	2580.99	0.66	5
Eastern	100	38.491	2764.34	2585.88	0.27	6
	102	37.857	104.36	2540.51	0.45	5

Table 9. Characteristics of seawater samples used for the reproducibility analysis. Average of calculated pH, along with standard deviations (STD) and number of samples collected from each Niskin (n).

4.4. DIC measurements

Sampling

DIC samples were collected in 500 mL borosilicate bottles, which were first rinsed and filled smoothly from the bottom. Water was overflow by at least half the volume of the bottle. They were stored at room temperature in the dark until analysis, maximum three days after sampled.

Analysis procedure and equipment

Analyses were performed with a *VINDTA 3D version#075* device coupled to a *UIC 5011* coulometer. The former device is designed and manufactured by the company *Marianda*. Samples were kept at laboratory temperature and stored at dark.

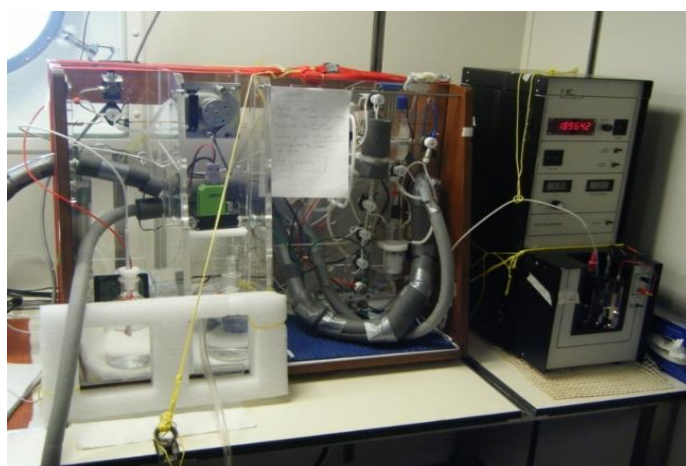


Figure 17. VINDTA system at the Trokenlabor in the R/V Maria S. Merian.

The sequence of steps followed for each session of analysis is shown in Table 10.

Step	Procedure
Junk	Seawater from the tap is titrated to start the system
Blank	The blank is calculated so the resto of the values can be obtained
<i>SW1</i>	Seawater from the tap is titrated to start the system*
<i>SUB1</i>	Substandard is analyzed to control drift along station and cruise*
<i>CRM1</i>	CRM is analyzed to check the accuracy*
<i>Samples</i>	The first, each six and the last sample of a DIC session are analyzed twice
<i>CRM1</i>	CRM is analyzed to check the system is working properly*
<i>SUB1 final</i>	Substandard is analyzed to control drift along station and cruise*

Table 10. Sequence of activities followed every session of DIC analysis. Replicates are conducted in steps in italics and marked with * in the procedure. Those replicates show the precision of the VINDTA system. If the difference between replicates is greater than 1 $\mu\text{mol/kg}$, a third measurement was performed. If it was smaller, analysis continued to the next step.

Quality control

Accuracy

In order to control the accuracy, a CRM was analyzed before and after every set of samples. The batch of the CRM, provided by Dr. Andrew Dickson was #158 and #170.

As for the TA, an additional control of accuracy was conducted by the analysis of substandard seawater at the beginning and at the end of each set of samples. The substandard corresponded to seawater from the minimum of salinity, at 700 m depth in St 2, collected at the beginning of the cruise and stored at dark.

The values of the substandard control are represented in Figure 18 and summarized in Table 11.

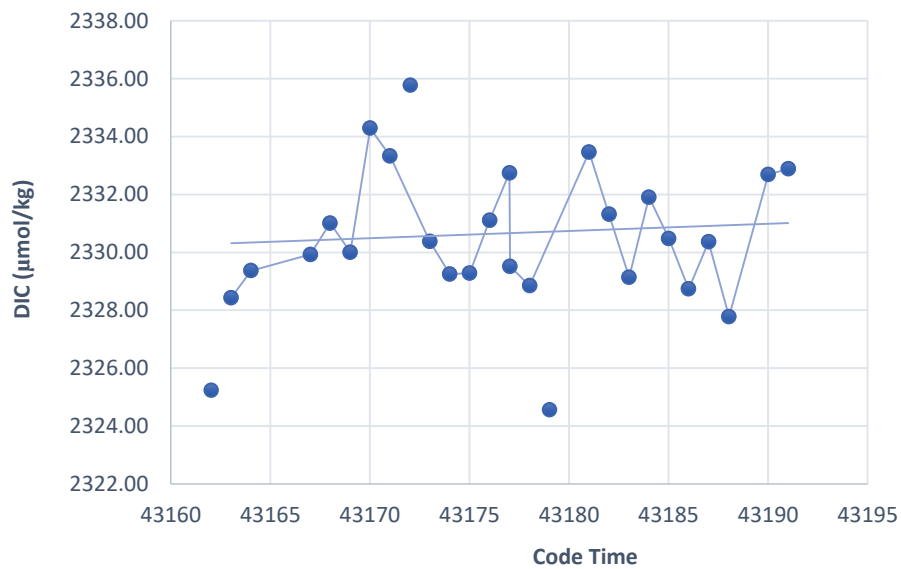


Figure 18. DIC values for the substandard seawater represented against code time.

Batch	Date	Stations	Calfactor	Fitted DIC	Mean SUB DIC	Av.DIC Dif
1	03/03/2018	1 2	1.003589	2 043.54±0.17	2 325.23±0.01	0.26 (5)
2	04/03/2018	2 4	1.004877	2 043.54±0.40	2 328.44±1.06	0.33 (5)
3	05/03/2018	8 9	1.004951	2 043.54±0.74	2 329.37±0.44	0.43 (2)
4	08/03/2018	13 17	1.005444	2 043.54±0.54	2 329.92	0.73 (4)
5	09/03/2018	17	1.005178	2 043.54±0.28	2 331.01±1.01	0.51 (1)
6	10/03/2018	17 23	1.003013	2 043.54±0.04	2 330.01±0.17	0.66 (5)
7	11/03/2018	23 30	1.003842	2 043.50±0.06	2 334.29±0.20	0.58 (3)
8	12/03/2018	30 34	1.005017	2 043.54±0.08	2 333.34±0.68	0.66 (1)
9	13/03/2018	34	1.004795	2 043.54±0.48	2 335.77±0.80	0.10 (2)
10	14/03/2018	38 40	1.003850	2 043.54±0.64	2 330.38±0.57	-
11	15/03/2018	40 47	1.002913	2 043.54±0.40	2 329.25±0.24	0.12 (1)
12	16/03/2018	40 51 52	1.001402	2 043.54±0.07	2 329.29±1.00	0.48 (5)
13	17/03/2018	51 55	1.002278	2 043.54±0.18	2 331.11±0.58	0.62 (3)
14	18/03/2018	55 56	1.003981	2 043.54±0.17	2 332.75±0.17	0.73 (2)
15	18/03/2018	59 63	1.003394	2 043.38±0.22	2 329.52±0.47	0.52 (3)
16	19/03/2018	68	1.001563	2 043.54±0.26	2 328.85±0.70	0.60 (3)
17	20/03/2018	72	1.000340	2 043.54±0.27	2 324.56±0.07	0.54 (4)
18	22/03/2018	77	1.004441	2 043.54±0.06	2 333.47±0.41	0.65 (10)
19	23/03/2018	83	1.003781	2 043.54±0.54	2 331.31±0.77	0.13 (2)
20	24/03/2018	83 87	1.002515	2 043.54±0.27	2 329.14±0.52	0.53 (5)
21	25/03/2018	91	1.003094	2 043.58±0.72	2 331.90±0.88	0.00 (0)
22	26/03/2018	97	1.001814	2 043.54±0.06	2 330.48±1.17	0.35 (4)
23	27/03/2018	100 102 105	1.002474	2 043.72±0.83	2 328.74	0.93 (1)
24	28/03/2018	105 109	1.002890	2 043.27±1.40	2 330.37±1.13	0.55 (7)
25	29/03/2018	109 113	1.000191	1 982.42	2 327.78±1.14	0.45 (4)
26	31/03/2018	113 121	1.002549	1 982.42±0.42	2 332.69±0.13	0.59 (3)
27	01/04/2018	130	1.001171	1 982.42±0.73	2 332.88±1.31	0.23 (2)

Table 11. Evaluation of the drift in the DIC measurements by analysis of a CRM and substandards. All DIC values in $\mu\text{mol/kg}$. CALFACTOR is the ratio between the certified DIC and the corresponding DIC determinations (batch #158 and #170 with a certified DIC of $2043.54 \pm 0.46 \mu\text{mol/kg}$ and $1982.42 \pm 0.68 \mu\text{mol/kg}$, respectively). The mean value of the DIC measurements on the CRM samples is shown (Fitted DIC \pm standard deviation). The mean value of the DIC measurements on the substandard samples is also shown (Mean SUB DIC \pm standard deviation). The average of the difference (Av. Dif. and number of duplicates) in the duplicate's analyses is also shown.

Precision

Again, five samples from the same Niskin bottle in four stations (two on each basin) were analyzed. Table 12 shows the mean DIC, standard deviation and number of analyzed samples.

Basin	St	Salinity	Depth (m)	DIC ($\mu\text{mol/kg}$)	STD	n
Western	52	38.727	3402.37	2309.50	0.63	5
	56	38.605	103.56	2279.53	0.40	4
Eastern	100	38.491	2764.03	2324.80	1.08	4
	102	38.045	104.75	2262.21	0.91	5

Table 12. Average value, standard deviation (STD) and number of samples collected for each DIC analysis at the chosen stations

In addition, duplicate analysis of samples were performed, one after the other every four or five samples.

4.5. CO₃²⁻ measurements

Sampling

The sampling procedure for carbonate ion is the same as the one previously explained in section 0 for pH, but samples are collected in quartz cuvettes instead of optical glass ones. It takes place after sampling for alkalinity determinations.

Analysis procedure and equipment

The method followed for determining the concentration of carbonate ion is the one proposed by Patsavas et al. ⁶, analogous to the one for pH determination, so the same equipment was used (Figure 11), but with different reactants and cells.

Samples were warmed in a thermostatic bath at 25°C, and for each measurement, a blank was performed. 20 µL of the indicator, in this case Pb(ClO₄)₂, the complexing agent were added to the sample with an adjustable pipette (Eppendorf Multipipette plus). Lead perchlorate was 0.022 M, prepared from the commercial product from Fisher Scientific, 99.99% pure, dissolving with distilled water.

After the addition of complexing agent, sample was shaken and absorbance was measured three times at three wavelengths: 234, 250 and 350 nm; isosbestic point of PbCO₃, wavelength presenting high absorbance variation and a non-absorbing wavelength respectively.

Quality control

First quality control

The processing of CO₃²⁻ data was similar to the explained for pH data. The same criteria were considered and same flags were given for errors.

Precision

A reproducibility test was also performed for carbonate determinations following the same process as for the other three parameters. Five samples were drawn from the same Niskin bottle at stations 52, 56, 100 and 105.

Basin	St	Depth (m)	CO ₃ ²⁻ (µmol/kg)	STD	n
Western	52	3402.37	226.6	1.0	5
	56	103.56	240.8	0.9	5
Eastern	100	2764.03	204.1	0.9	5
	102	104.75	238.4	0.4	5

Table 13. Average CO₃²⁻ concentration value of the n number of samples with the corresponding standard deviation (STD) and respective stations and depths.

RESULTS AND DISCUSSION

5.1. pH controversy: measurements with pure vs. unpurified m-cresol

As a brief reminder, the method followed for determining pH consists on spectrophotometric analysis of the seawater samples before and after the addition of the indicator dye, m-cresol purple (m-CP).

In 2007, Yao et al.²⁶ found some impurities in the m-CP that absorb at 434 nm, (wavelength corresponding to the basic form maximum of absorbance), therefore in higher ranges of pH, the obtained values are lower than their corresponding real values.

This issue has been studied by several authors^{19,28} and different solutions have been proposed, to either purify the m-CP, or to correct the pH obtained from unpurified indicator (pH_{UNPUR}) by comparison with pH calculated using pure indicator (pH_{PUR}). These do not eliminate the problem completely, since purified indicator is more expensive, and some laboratories may not be able to afford neither the purified m-CP nor the instruments required to purify it.

Being aware of the importance of CO₂ measurements (1.3, page 14), seems logic and necessary the consistency between values obtained in different laboratories around the world.

In 2015, Bockmon and Dickson²⁷ studied the actual quality of discrete seawater CO₂ measurements (AT, DIC and pH) through an inter-laboratory exercise. Two batches A and B were used for this comparison, and the conclusion for pH was that for Batch A, more than half laboratories had an accuracy of 0.01 pH units, while for Batch B only about a third did.²⁷

Figure 19 was extracted from the article on this inter-laboratory comparison and shows the difference between the pH values reported by the different laboratories and the certified pH value with purified dye.

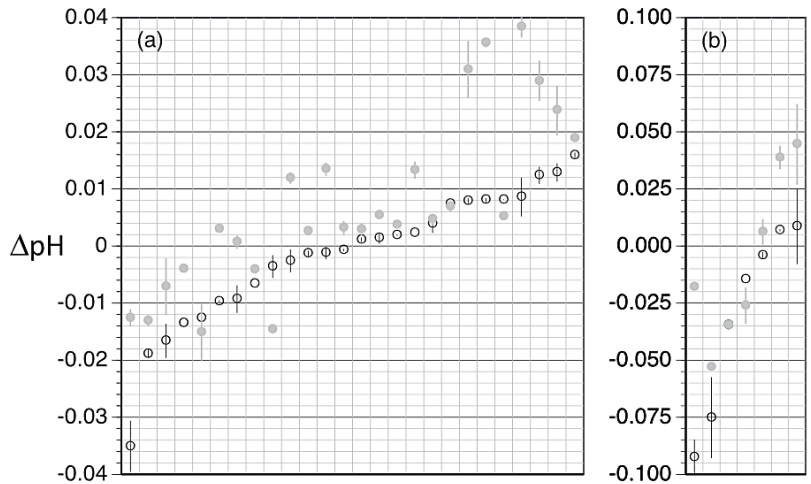


Figure 19. Differences between the pH values (25°C, total scale) reported by different laboratories participating in an inter-laboratory comparison. Batch A is represented in black and batch B in solid gray. (a) corresponds to values obtained through spectrophotometric techniques, and (b) through electrometric techniques. (Bockmon and Dickson, 2015).

During MSM72, the pH of 9 stations was measured using both purified and unpurified m-CP. The difference between pH_{UNPUR} and pH_{PUR} (both 25°C, total scale is represented against the depth at which the sample was taken in Figure 19. **No se encuentra el origen de la referencia.** pH_{UNPUR} values were obtained following the recommendations by Clayton and Byrne¹⁸ (mentioned above, section 3.1) while pH_{PUR} values were calculated following the equations by Liu et al.²⁸

The main conclusion from those sets of analysis is that it does not seem to be any apparent difference between using purified or unpurified m-CP in the MedSea waters, because the pH values are under the uncertainties of pH methodologies.

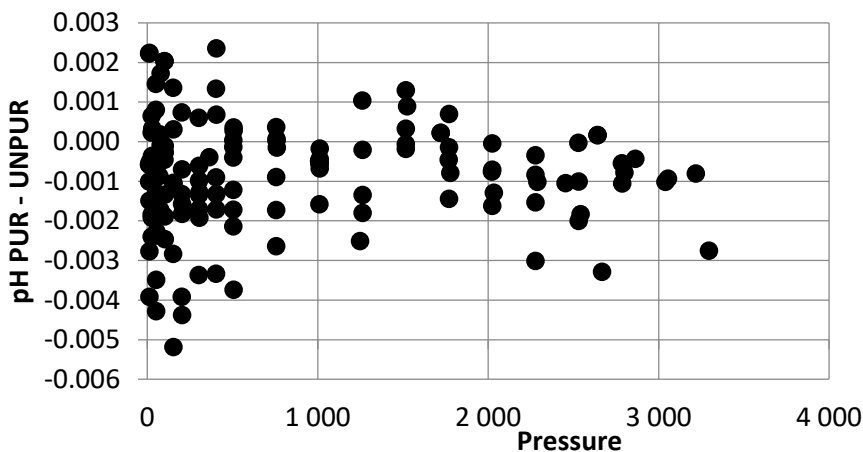


Figure 20. Difference between pH (25°C, total scale) obtained using purified and unpurified m-CP indicator.

5.2. CO₂ internal consistency

Knowing two of the measurable variables of the system (pH, TA, DIC, pCO₂ and also CO₃²⁻) it is possible to calculate the remaining variables using the thermodynamic equations of the CO₂ system in seawater and the corresponding constants, so the whole system can be known. As our group measured four out of five parameters, the internal consistency of the measurements can be studied.

The calculated derived CO₂ variables are obtained using the CO2SYS package with the dissociation constants given by Lueker²⁹ in 2000 and the B/Cl ratio proposed by Lee³⁰ in 2010

DIC

The residuals of DIC (Δ DIC) were estimated as the measured DIC values minus the calculated from TA and pH measured.

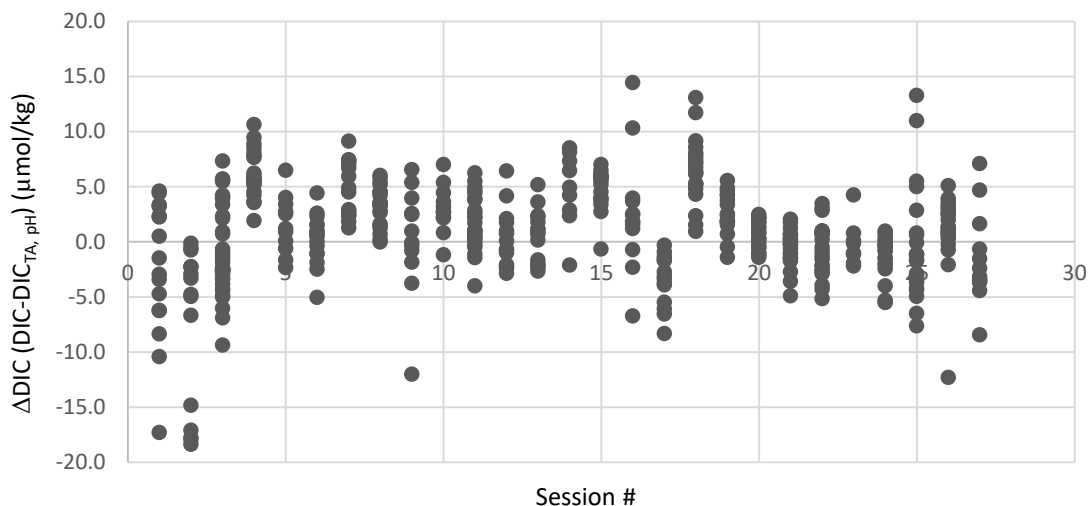


Figure 21. Residuals of DIC (Δ DIC) obtained as DIC measured minus DIC calculated from TA and pH .

In Figure 21, the Δ DIC obtained from MSM72 cruise are represented regarding the number of station. The majority of the residuals are between $\pm 5 \mu\text{mol/kg}$. Then, there are many in the $\pm 10 \mu\text{mol/kg}$ range, and sporadically some residuals are higher than $10 \mu\text{mol/kg}$.

Considering these results, it is possible to say that our MSM72 CO₂ system is internally consistent in terms of pH, TA and DIC.

CO_3^{2-}

In the case of CO_3^{2-} , residuals ($\Delta[\text{CO}_3^{2-}]$) were calculated as the difference between the measured and the calculated $[\text{CO}_3^{2-}]$ from pH and TA. In **¡Error! No se encuentra el origen de la referencia.** $\Delta[\text{CO}_3^{2-}]$ are represented by stations.

As it can be observed in **¡Error! No se encuentra el origen de la referencia.**, the smaller residual has a value of $10 \mu\text{mol/kg}$, being most of them between 20 and $40 \mu\text{mol/kg}$.

The reason for this discrepancy is currently being studied at the IEO of A Coruña. An initial hypothesis aims for the degradation of the complexing agent with time, but looking at $[\text{CO}_3^{2-}]$ results obtained using the same reactant during different studies within the coastal area of Ría de A Coruña, the error seems to be kept throughout the months.

Another hypothesis could be that the method is not appropriate for these kind of waters, maybe due to the high salinities of Mediterranean Sea. The MSM72 cruise was the first time this method was applied to analyze natural waters of such characteristics as the Mediterranean's, very different to those used to optimize the method.

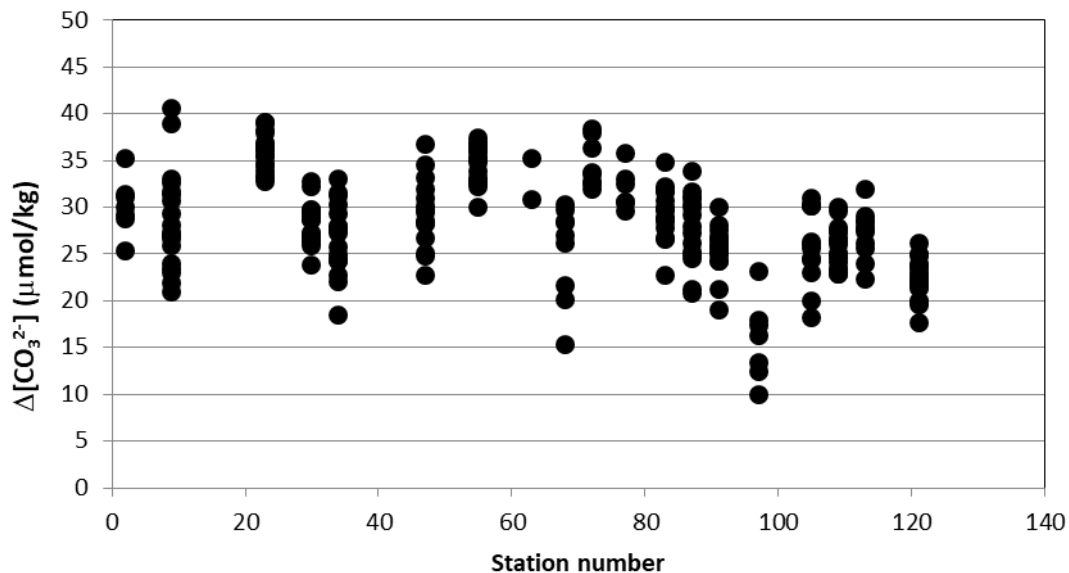


Figure 22. Residuals for carbonate ion. $\Delta[\text{CO}_3^{2-}]$ is the difference between the measured $[\text{CO}_3^{2-}]$ and the $[\text{CO}_3^{2-}]$ calculated from pH and TA

5.1. Basin wide vertical distributions in relation to water masses

Once all the CO₂ variables for the MSM72 cruise were measured and the whole CO₂ database passed the first quality control, they can be plotted in order to see their distributions along the Mediterranean basins and to extract information from them. In this section, the CO₂ system variables will be studied in reference to space, in order to look for information about the CO₂ system basin-wide state, and the Mediterranean water masses.

Salinity, temperature and oxygen

In order to differentiate among the different water masses of the Mediterranean Sea, the vertical distributions of salinity and temperature together with the dissolved oxygen are shown.

In Figure 23, the Atlantic Water (AW) can be easily recognized entering the Western basin at the top, with the lowest salinities (~37.5 down to 36), and low temperatures that increase eastward as the water is closer to the surface and mixing with warmer waters.

The Western-Mediterranean Deep Water (WMDW) is observed as a more homogeneous cold-water mass, with temperatures below 14°C and higher salinities, around 38.5. Likewise, the Eastern-Mediterranean Deep Water (EMDW) coming from the Adriatic in pre-EMT conditions and from the Aegean during EMT, has even higher salinities (~38.6) and slightly higher temperatures (around 14°C)

Finally, Levantine Intermediate Water (LIW) is also easy to locate in. Its temperatures and salinities are the highest (over 15°C, up to 17°C; and from 39 up respectively). Its entrance into the Western basin is also noticeable in Figure 23.

Regarding the dissolved oxygen, the oxygen concentration follows a general trend, having a maximum at the surface, decreasing during the first 1000 m and then increasing again below that depth due to the biological activity, located in the intermediate layers. The minimum oxygen content can be observed in the western basin.

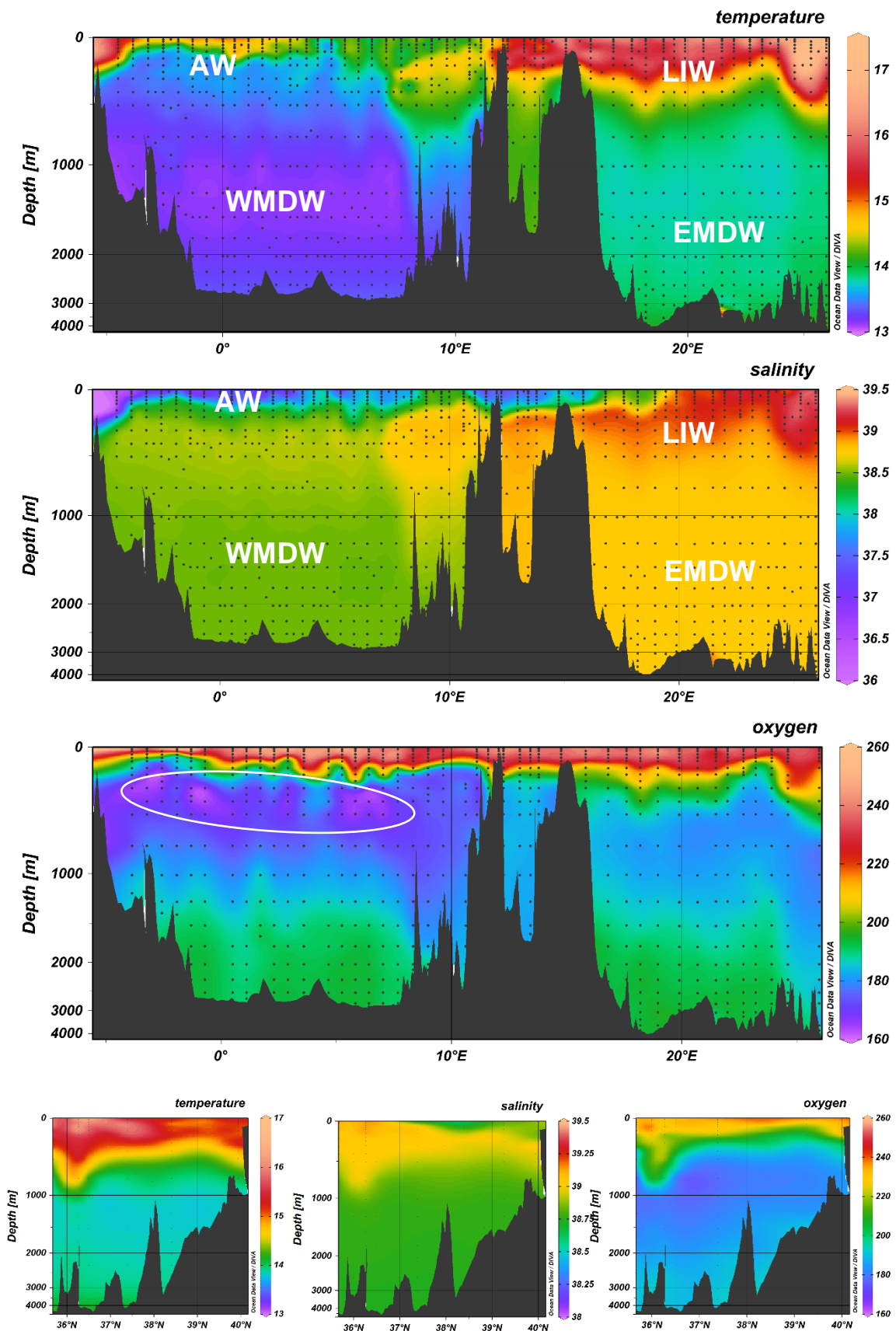


Figure 23. Vertical distribution of Temperature ($^{\circ}\text{C}$), salinity (spU) and oxygen ($\mu\text{mol/kg}$) longitudinal section of the Mediterranean Sea, data from the MSM72 cruise in 2018. Water masses are labeled in white, and the water with minimum content in oxygen is circled. At the bottom, latitudinal sections of the three parameters.

CO₂ variables

For the CO₂ variables, three images will be shown per parameter: (a) the top one will be a longitudinal section from Crete to the Strait of Gibraltar, (b) the bottom left will be a reference map, with the stations marked as blue squares and the longitudinal section West-East marked in red, and (c) the bottom right will be a latitudinal section South-North of the transect from the Adriatic to the Ionian basins inside the Eastern basin.

The colour scale key will be located on the right of each plot. In all cases, the top depths will be stretched since water properties vary more than at the more homogeneous bottom. Sampled depths are marked as black dots.

TA

The alkalinity profile is very similar to that obtained for salinity; all mentioned water masses can be easily localized. The distribution of alkalinity and salinity coincide, being the AW the less alkaline water mass, followed by the WMDW, the EMDW and finally the most alkaline LIW (Figure 24).

The AW comes from the Strait of Gibraltar with the lower values of TA (>2450 $\mu\text{mol/kg}$) entering until the Eastern basin, in which the TA values increase until the 2500 $\mu\text{mol/kg}$ (Figure 24a).

The core of the LIW is observed in Figure 24(a) as the maximum of TA with values of 2650 $\mu\text{mol/kg}$, entering westward until the connexion with the Thyrrenian Sea, where it signal starts to diluted. In Figure 24(c), the LIW can also be recognized as a highly alkaline mass in the first 1000 m.

The heterogeneity of the upper layers is accused in the representations of this variable, which covers a wide range of TA values (from below 2400 to almost 2600 $\mu\text{mol/kg}$) in the first 500 m. On the contrary, the TA of deep water masses is kept constant from above 1500 m to the bottom (mean bottom depth 3000 m for the Western and around 4000 m for the Eastern basin) with values around 2550 $\mu\text{mol/kg}$ and 2625 $\mu\text{mol/kg}$ at the Western and Eastern basin, respectively.

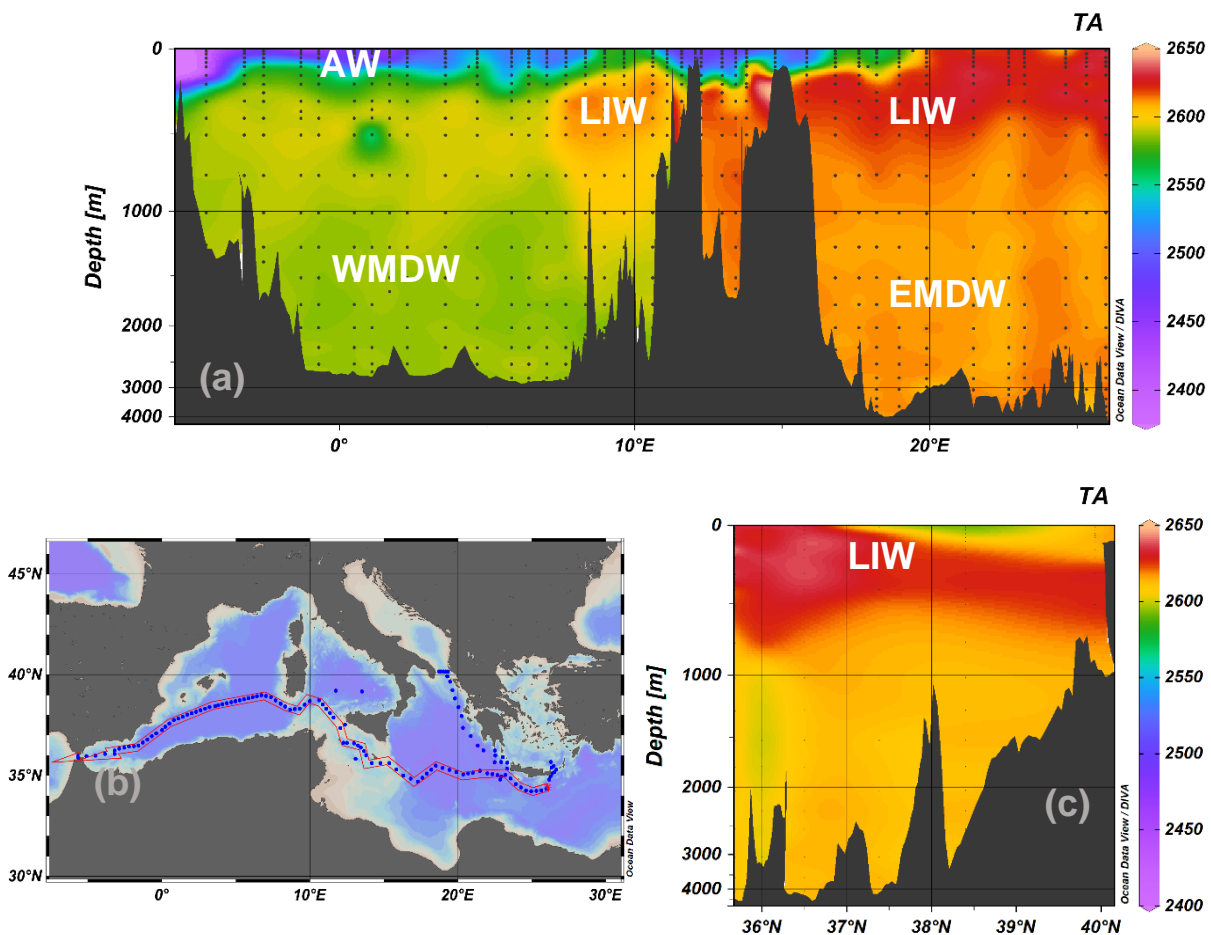


Figure 24. (a) Longitudinal TA section. (b) reference MedSea map. (c) Latitudinal view of TA from Adriatic to Ionian Sea. Cruise MSM72, 2018.

pH

A clear difference regarding pH distribution between basins can be observed in Figure 25(a), belonging to the Western basin the lowest values. Also, values corresponding to deeper water show high homogeneity, while those from the surface vary very rapidly.

In the Western basin, the pH decreases from top to bottom except for the area closest to the Strait of Gibraltar, where a minimum of 7.85 pH units is shown, but it goes up to 7.97 in around 100 m towards the surface.

The Eastern basin, on the other hand shows a totally different trend. The EMDW has a pH of around 7.96, which decreases gradually towards the surface, until around 500 m depth, where it reaches a pH of 7.93. Then it starts decreasing again up until 250 m, with a pH similar to the bottom one, to then suddenly increase up to a pH of 8.

In conclusion, there is a highly basic upper layer (7.96-8) and a slightly less basic deep water (7.96-7.93).

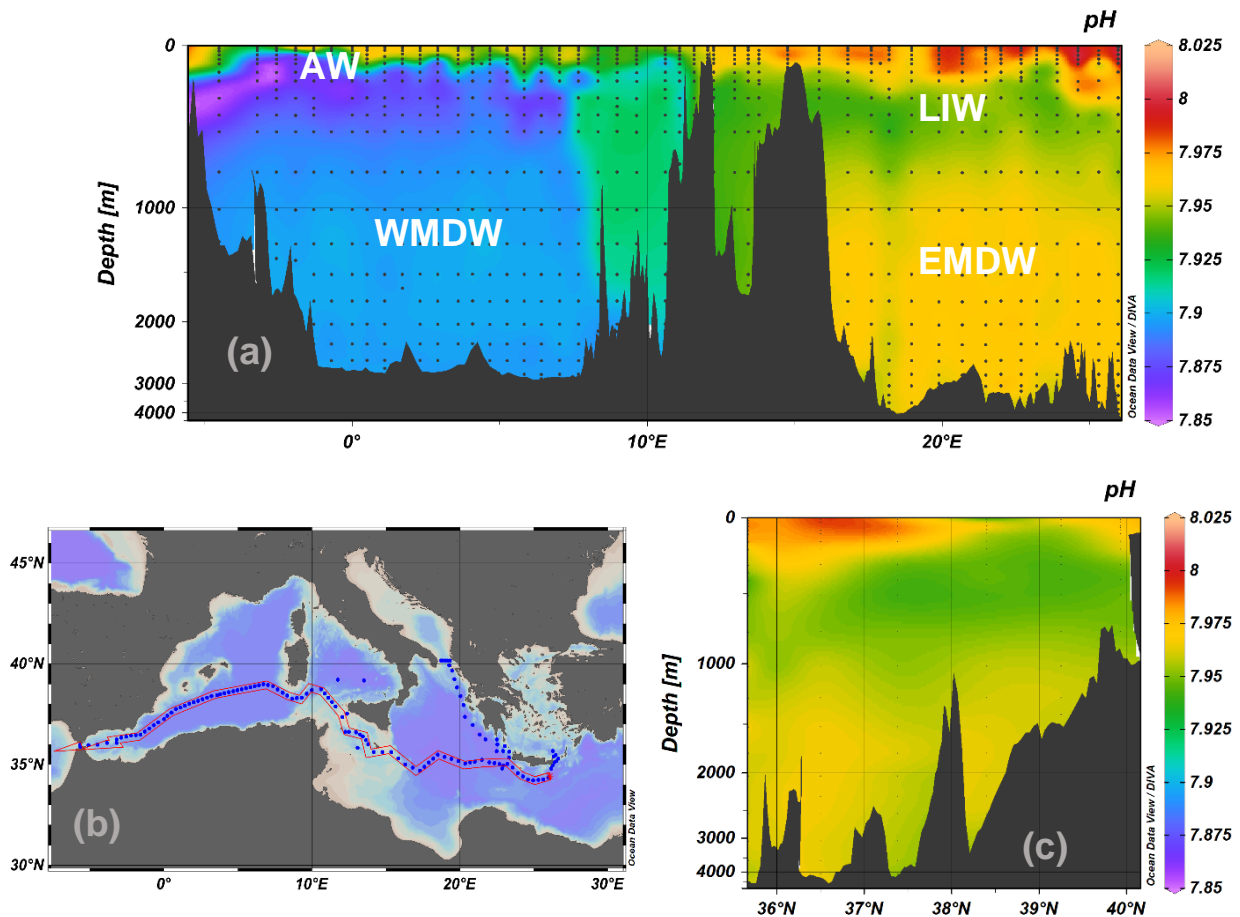


Figure 25. a) Longitudinal pH section. (b) reference MedSea map. (c) Latitudinal view of pH from Adriatic to Ionian Sea. Cruise MSM72, 2018.

DIC

In the Figure 26(a), upper waters show considerable difference of DIC with deep waters. The AW enters the MedSea with relatively low DIC values (~2150-2250 $\mu\text{mol/kg}$), which start increasing when it reaches the Strait of Sicily. In the Eastern basin, the maximum of DIC is detected related to the LIW with DIC content of 2350 $\mu\text{mol/kg}$.

The deep waters (WMDW and EMDW) show relatively high values of DIC that keep quasi homogenous at the Western basin (~2325 $\mu\text{mol/kg}$) and slightly lower DIC values around 2300 $\mu\text{mol/kg}$ at the Eastern basin.

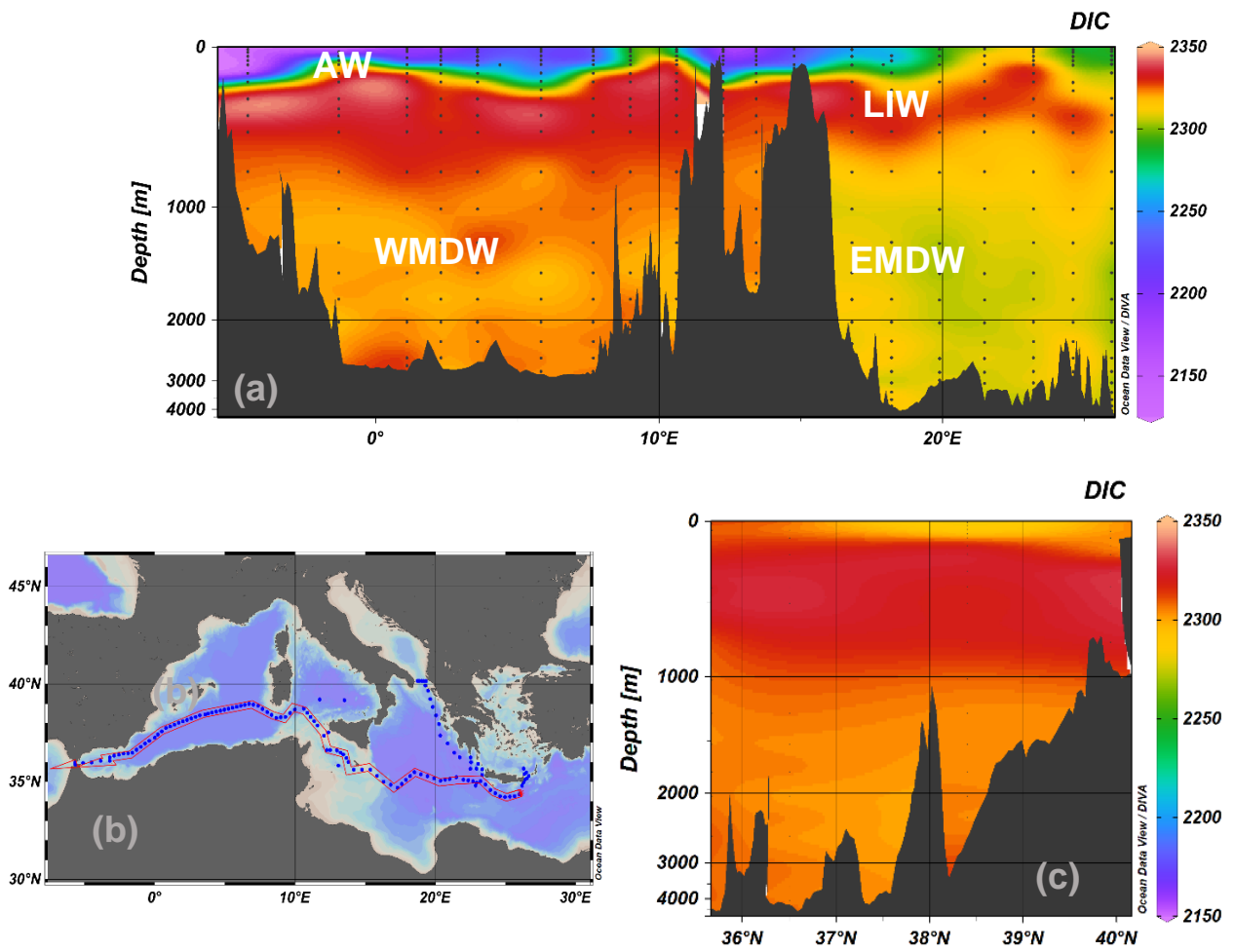


Figure 26. a) Longitudinal DIC section. (b) reference MedSea map. (c) Latitudinal view of DIC from Adriatic to Ionian Sea. Cruise MSM72, 2018.

CONCLUSIONS

From the direct participation in the MSM72 cruise as part of the IEO group responsible of CO₂ measurements, and the onboard analysis and posterior quality control of database processes, the main conclusion this TFG are:

- Due to the importance of the CO₂ system in seawater and particularly in the Mediterranean Sea, it is of crucial importance the whole procedure, from the taking of samples, the adequately storage to the analysis itself. One mistake in either step, could mean the loss of data points in the quality control procedures.
- Taking into account the state of the art of pH methodology, it seems complicate to select the proper equations. In this TFG, the comparison between unpurified (pH_{UNPUR}) and pure (pH_{PUR}) m-cresol purple was made for the first time. The result of that comparison does not show any apparent difference between using pH_{UNPUR} and pH_{PUR}, at least in the MedSea where both pH methodologies are close to the upper range of application.
- The good quality CO₂ database of the MSM72 was demonstrated by the precision and accuracy measurements. In addition, an internal consistency study was made in terms of DIC to ensure that the CO₂ database of MSM72 is internally consistent.
- The main water masses in the Mediterranean Sea are the Atlantic Water (AW), the Levantine Intermediate Water (LIW), and the Western and Eastern Mediterranean Deep Waters (WMDW and EMDW, respectively). These water masses can be identified by their temperature and salinity. In addition, it is possible to relate those water masses with the biogeochemical properties (O₂, TA, pH and DIC) through the study of their distributions.

APPENDIX

TABLE 14: Relation of samples collected at each station for sampled parameters

ST	DEPTH	DIC	PH	TA	CO ₃ ²⁻
1	313	5	5	5	
2	2368	19	19	19	19
4	741	14	14	14	
8	1150	14	14	14	
9	3700	23	46	23	23
11	3450		21	15	
13	3000	20	20	20	
15	3000		19		
17	3100	21	21	21	
20	400		9	9	
22	2928		20	20	
23	4603	19	22	22	22
26	3200		22	22	
30	4100	19	22	22	22
32	4200		22	14	
34	2500	18	19	19	19
36	1400		15		
38	1000	11	13	13	
39	950		10		
40	1000	10	15	10	
41	950		11		
42	800		14	9	
43	500	8	11	11	
44	3300		24	22	24
46	3200		21		
47	3400	17	48	21	21
49	2800		22		
51	3000	16	22	20	
52	3200	5	10	5	5
53	3800		24	22	
55	4000	20	24	22	22
56	3600	5	10	5	5
57	2800		44	20	
59	2200	14	19	17	
61	500		12	10	
63	500	4	14	6	6
66	1100		14	14	
68	1800	16	32	16	16
70	1000		13	13	
72	1400	14	14	14	14
73	100		5	5	
75	3500		21	21	
77	3200	21	42	21	21

79	500		10	10	
81	800		11	11	
83	2600	19	19	19	19
85	1800		16	16	
87	2200	19	19	19	19
89	2100		24	22	
91	2900	20	40	20	20
93	2800		20	20	
95	2900		20	20	
97	2800	21	21	21	21
99	2800		23		
100	2700	5	10	5	5
101	2600		19	19	
102	2500	5	10	5	
103	2500		19		
105	2600	18	30	18	23
107	2600		22		
109	2500	19	21	19	19
111	1500		15	15	
113	2600	19	37	19	19
115	2600		19	19	
117	2600		19		
119	2600		19	19	
121	2500	18	36	16	18
123	1350		12		
125	1340		24	12	
128	1300		12	12	
130	1300	13	26	13	13
132	600		9	9	
134	350		9	9	
136	500		10	10	

TOTAL	DIC	pH	TA	CO ₃ ²⁻
	509	1440	973	415

Table 14. Relation of stations, their maximum depth and number of samples taken for each parameter.

Bibliography

- (1) Zeebe, R. E.; Wolf-Gladrow, D. *CO₂ in Seawater: Equilibrium, Kinetics, Isotopes*; 2002; Vol. 36.
- (2) Wedborg, M.; Turner, D. R.; Anderson, L. G.; Dyrssen, D. Determination of PH. In *Methods of Seawater Analysis*; Kiel.
- (3) Dickson, A. G.; Sabine, C. L.; Christian, J. R. Guide to Best Practices for Ocean CO₂ Measurements. *PICES Spec. Publ.* **2007**, 3 (8), 191.
- (4) Anderson, L. G.; Turner, D. R.; Wedborg, M.; Dyrssen, D. Determination of Total Alkalinity and Total Dissolved Inorganic Carbon. *Methods Seawater Anal.* **1999**, 1999, 127–148.
- (5) Fajar, N. M.; García-Ibáñez, M. I.; SanLeón-Bartolomé, H.; Álvarez, M.; Pérez, F. F. Spectrophotometric Measurements of the Carbonate Ion Concentration: Aragonite Saturation States in the Mediterranean Sea and Atlantic Ocean. *Environ. Sci. Technol.* **2015**, 49 (19), 11679–11687.
- (6) Patsavas, M. C.; Byrne, R. H.; Yang, B.; Easley, R. A.; Wanninkhof, R.; Liu, X. Procedures for Direct Spectrophotometric Determination of Carbonate Ion Concentrations: Measurements in US Gulf of Mexico and East Coast Waters. *Mar. Chem.* **2015**, 168, 80–85.
- (7) Easley, R. A.; Patsavas, M. C.; Byrne, R. H.; Liu, X.; Feely, R. A.; Mathis, J. T. Spectrophotometric Measurement of Calcium Carbonate Saturation States in Seawater. *Environ. Sci. Technol.* **2013**, 47, 1468–1477.
- (8) Raven, J. A.; Falkowski, P. G. Oceanic Sinks for Atmospheric CO₂. **1999**, 741–755.
- (9) Robinson, A. R.; Leslie, W. G.; Theocharis, A.; Lascaratos, A. Mediterranean Sea Circulation. In *Encyclopedia of Ocean Sciences: Second Edition*; 2008; pp 710–725.
- (10) Egleston, E. S.; Sabine, C. L.; Morel, F. M. M. Revelle Revisited: Buffer Factors That Quantify the Response of Ocean Chemistry to Changes in DIC and Alkalinity. *Global Biogeochem. Cycles* **2010**.
- (11) Varela, R. A.; Rosón Porto, G. *Métodos En Oceanografía Física*; Anthias, Ed.; 2008.
- (12) Emery, W. J. *Water Types and Water Masses*. **2003**.
- (13) Tsimplis, M. N.; Zervakis, V.; Josey, S. A.; Peneva, E. L. Changes in the Oceanography of the Mediterranean Sea and Their Link to Climate Variability. In *The Atlantic and Mediterranean Sea as connected system*; 2006.
- (14) Tanhua, T.; Hainbucher, D.; Schroeder, K.; Cardin, V.; Álvarez, M.; Civitarese, G. The Mediterranean Sea System: A Review and an Introduction to the Special Issue. *Ocean Science*. 2013.
- (15) Tanhua, T.; Hainbucher, D.; Cardin, V.; Civitarese, G.; McNichol, A. P.; Key, R. M.; Hole, W.; Program, O. S. Repeat Hydrography in the Mediterranean Sea, Data from the Meteor Cruise 84/3 in 2011. **2013**, 289–294.
- (16) Kitack, L.; Sabine, C. L.; Tanhua, T.; Kim, T.-W.; Feely, R. A.; Kim, H.-C. Roles of Marginal Seas in Absorbing and Storing Fossil Fuel CO₂. *Energy Environ. Sci.* **2011**, 4, 1133–1146.

- (17) Schroeder, K.; Tanhua, T.; Bryden, H. L.; Álvarez, M.; Chiggiato, J.; Aracri, S. Mediterranean Sea Ship-Based Hydrographic Investigations Program (Med-SHIP). *Oceanography* **2015**, *28*(3):12–1, 12.
- (18) Clayton, T. D.; Byrne, R. H. Spectrophotometric Seawater PH Measurements: Total Hydrogen Ion Concentration Scale Calibration of m-Cresol Purple and at-Sea Results. *Deep. Res. Part I* **1993**, *40* (10), 2115–2129.
- (19) Loucaides, S.; Rèrolle, V. M. C.; Papadimitriou, S.; Kennedy, H.; Mowlem, M. C.; Dickson, A. G.; Gledhill, M.; Achterberg, E. P. Characterization of Meta-Cresol Purple for Spectrophotometric PH Measurements in Saline and Hypersaline Media at Sub-Zero Temperatures. *Sci. Rep.* **2017**, *7* (1), 1–11.
- (20) Grasshoff, K.; Kremling, K.; Ehrhardt, M.; Anderson, L. G.; Andreae, M. O.; Behrens, B.; van den Berg, C.; Brüggemann, L.; Burns, K. A.; Cauwet, G.; et al. *Methods of Seawater Analysis*. **1999**, 1–600.
- (21) Perez et Al Improvements in Alkalinity *Ciencias Marinas* 2000 26(3) 463-478.Pdf.
- (22) Dickson, A. G. The Measurement of Sea Water PH. In *Marine Chemistry*, 1993; Vol. 44, pp 131–142.
- (23) Johnson, K. M.; Wills, K. D.; Butler, D. B.; Johnson, W. K.; Wong, C. S. Coulometric Total Carbon Dioxide Analysis for Marine Studies: Maximizing the Performance of an Automated Gas Extraction System and Coulometric Detector. *Mar. Chem.* **1993**, *44* (2–4), 167–187.
- (24) Byrne, R. H.; Yao, W. Procedures for Measurement of Carbonate Ion Concentrations in Seawater by Direct Spectrophotometric Observations of Pb(II) Complexation. *Mar. Chem.* **2008**, *112* (1–2), 128–135.
- (25) Knudsen's pipette <https://glossary.periodni.com> (accessed Jul 19, 2018).
- (26) Yao, W.; Liu, X.; Byrne, R. H. Impurities in Indicators Used for Spectrophotometric Seawater PH Measurements: Assessment and Remedies. *Mar. Chem.* **2007**, *107* (2), 167–172.
- (27) Bockmon, E. E.; Dickson, A. G. An Inter-Laboratory Comparison Assessing the Quality of Seawater Carbon Dioxide Measurements. *Mar. Chem.* **2015**, *171*, 36–43.
- (28) Liu, X.; Patsavas, M. C.; Byrne, R. H. Purification and Characterization of Meta Cresol Purple for Spectrophotometric Seawater PH Measurements. *Environ. Sci. Technol.* **2011**, *45* (11), 4862–4868.
- (29) Lueker, T. J.; Dickson, A. G.; Keeling, C. D. Ocean PCO₂ Calculated from Dissolved Inorganic Carbon, Alkalinity, and Equations for K₁ and K₂: Validation Based on Laboratory Measurements of CO₂ in Gas and Seawater at Equilibrium. *Mar. Chem.* **2000**, *70* (1), 105–119.
- (30) Lee, K.; Kim, T. W.; Byrne, R. H.; Millero, F. J.; Feely, R. A.; Liu, Y. M. The Universal Ratio of Boron to Chlorinity for the North Pacific and North Atlantic Oceans. *Geochim. Cosmochim. Acta* **2010**, *74* (6), 1801–1811.